TM X-56030

EXPLORATORY WIND TUNNEL TESTS OF A SHOCK-SWALLOWING AIR DATA SENSOR AT A MACH NUMBER OF APPROXIMATELY 1.83

Jack Nugent (Flight Research Center), Lana M. Couch (Langley Research Center), and Lannie D. Webb (Flight Research Center)

March 1975

NASA Flight Research Center
Edwards, California 93523

1. Report No.	2. Government Accession No.	3. Recipient's Catalog No.
TM X-56030		

4. Title and Subtitle	5. Report Date
EXPLORATORY WIND TUNNEL TESTS OF A SHOCK-SWALLOWING AIR DATA SENSOR AT A MACH NUMBER OF APPROXIMATELY 1.83	March 1975
	6. Performing Organization Code H-885

7. Author(s)	8. Performing Organization Report No.
Jack Nugent (Flight Research Center), Lana M. Couch (Langley Research Center), and Lannie D. Webb (Flight Research Center)	
	10. Work Unit No. 505-06-23
9. Performing Organization Name and Address	11. Contract or Grant No.
NASA Flight Research Center P. O. Box 273 Edwards, California 93523	
	13. Type of Report and Period Covered Technical Memorandum
12. Sponsoring Agency Name and Address	14. Sponsoring Agency Code
National Aeronautics and Space Administration Washington, D. C. 20546	

15. Supplementary Notes

16. Abstract

The test probe was designed to measure free-stream Mach number and could be incorporated into a conventional airspeed nose boom installation. Tests were conducted in the Langley 4- by 4-Foot Supersonic Pressure Tunnel with an approximate angle of attack test range of -5° to 15° and an approximate angle of sideslip test range of ±4°.

The probe incorporated a variable exit area which permitted internal flow. The internal flow caused the bow shock to be swallowed. Mach number was determined with a small axially movable internal total pressure tube and a series of fixed internal static pressure orifices. Several probe tips were tested.

Mach number error was at a minimum when the total pressure tube was close to the probe tip. For four of the five tips tested, the Mach number error derived by averaging two static pressures measured at horizontally opposed positions near the probe entrance were least sensitive to angle of attack changes. The Mach number error so derived was comparable to the errors obtained from conventionally designed airspeed sensors. The same orifices were also used to derive parameters that gave indications of flow direction.

17. Key Words (Suggested by Author(s))	18. Distribution Statement
Shock-swallowing probe Air data sensor Supersonic flow	Unclassified - Unlimited STAR Category: 06

19. Security Classif. (of this report)	20. Security Classif. (of this page)	21. No. of Pages	22. Price*
Unclassified	Unclassified	40	

For sale by the National Technical Information Service, Springfield, Virginia 22151

EXPLORATORY WIND TUNNEL TESTS OF A SHOCK-SWALLOWING AIR DATA SENSOR AT A MACH NUMBER OF APPROXIMATELY 1.83

Jack Nugent
Flight Research Center

Lana M. Couch
Langley Research Center

and

Lannie D. Webb
Flight Research Center

INTRODUCTION

Providing accurate air data measurements for high-speed aircraft during flight research programs requires considerable test effort. Extensive wind tunnel and flight tests are often made to obtain ambient static pressure and Mach number calibrations to cover the wide flight regimes of research aircraft (refs. 1 and 2). Several onboard sensors were needed to determine air data parameters during the X-15 program because no single onboard air data sensor available provided reliable air data parameters over the speed and altitude ranges tested (ref. 1). The flight regimes predicted for future research aircraft are even wider (ref. 3); consequently, there is a continuing need for the investigation and evaluation of new sensors.

A sensor that may be useful for air data measurements at supersonic and hypersonic speeds is a probe that permits enough air to flow through it to cause the normal shock wave to lie inside instead of in front of the probe. Probes of this type, which are called shock-swallowing probes, have been used in wind tunnels and arc-jets to measure mass flux and other free-stream flow parameters (refs. 4 and 5). The purpose of this report is to present the results of a brief exploratory wind tunnel test which evaluated the feasibility of using a shock-swallowing air data probe for high-speed aircraft. The probe was designed to measure free-stream Mach number by measuring internal total and static pressure and could be incorporated into a conventional airspeed nose boom installation. The investigation was conducted in the Langley 4- by 4-Foot Supersonic Pressure Tunnel.

SYMBOLS AND ABBREVIATIONS

M	Mach number
ΔM	Mach number error, M_∞ - local Mach number
p	static pressure
p_t	total pressure
Re	Reynolds number
α	angle of attack
β	angle of sideslip
Subscripts:	
∞	tunnel free-stream condition
i	internal total pressure tube
301,303,307	static pressure orifices

TEST PROBES AND VARIABLES

The essential difference between the operation of a conventional airspeed probe and that of a shock-swallowing probe is shown in figure 1. With a conventional probe (ref. 6) there is no internal flow. At supersonic speeds total pressure is sensed behind the probe's bow shock, and static pressure is sensed by means of external static pressure orifices downstream of the probe tip. Mach number is determined from these two measurements. As speed increases, the probe bow shock bends backward and increasingly tends to influence the static pressure sensed at the external orifices.

With the shock-swallowing probe, there are openings or exit areas near the rear of the probe and air is permitted to flow through the probe. This permits the bow shock to be swallowed. There is a series of static pressure ports inside the probe as well as a small total pressure tube. Mach number is determined from the internal total pressure and static pressure measurements. The effect of the external shock at the probe tip on the internal static pressures should not be as great as the effect of the bow shock on the external orifices of the conventional probe. Hence, static pressure and Mach number should be close to free-stream values.

One of the variables explored in the feasibility test was the exit area necessary to cause and maintain the swallowing of the shock. Another was the longitudinal position of the internal total pressure tube that resulted in the lowest Mach number

error. The location of the internal static pressure orifices that resulted in the most accurate Mach number calculation was also explored: it was suspected that static pressures measured near the probe tip would be closer to free-stream values than static pressures measured downstream in the probe, where they could be expected to be influenced by the internal shock system. Finally, five different probe tips were tested to determine the effect of the probe tip shape on the data.

The probe (fig. 2) was designed to swallow shocks at Mach numbers greater than approximately 1.1. In figure 2(a), the external sleeve that regulates the exit area is shown in the minimum area position; figure 2(b) shows the external sleeve in the maximum area or wide-open position. (The exit area consists of four oval slots, only two of which are visible.) In the wide-open position, the exit area is approximately four times the probe entrance area. Figure 3 is a drawing of the test probe in the wide-open sleeve position and shows the probe's movable internal total pressure tube and the tips tested.

WIND TUNNEL AND TEST CONDITIONS

The Langley 4- by 4-Foot Supersonic Pressure Tunnel is a continuous-flow tunnel with a total pressure range from 1.38 N/cm^2 to 17.2 N/cm^2 (2.0 psi to 25.0 psi) at a constant total temperature of approximately 317 K (570° R). Discrete Mach numbers from 1.41 to 2.20 can be obtained by using interchangeable nozzle templates.

The investigation was conducted at a free-stream Mach number of approximately 1.83 and at total pressures of 6.9 N/cm^2, 10.4 N/cm^2, and 13.8 N/cm^2 (10 psi, 15 psi, and 20 psi). Total temperature was held at 317 K (570° R). The range of angle of attack was approximately -5° to 15° and the range of angle of sideslip was approximately ±4°. Reynolds number ranged from approximately 8.2×10^6 per meter (2.5×10^6 per foot) to approximately 16.4×10^6 per meter (5×10^6 per foot). Figure 4 shows the probe in the wind tunnel.

TEST PROCEDURE

Two other pitot-static pressure probes were used during the investigation to determine as closely as possible the actual free-stream Mach number at the location of the experimental probe (fig. 4). One pitot-static probe was attached in the manner of an outrigger to the support for the experimental probe, so that the two probes were parallel and could be simultaneously traversed across the test section and varied in angle of attack and angle of sideslip. Since this pitot-static probe was mounted on the side of and with sufficient separation from the experimental probe, there was no flow-field interference between the probes over the angle of attack and angle of sideslip ranges tested. The other pitot-static probe, which was also mounted in the free-stream flow, was fixed to a bracket mounted on the wind tunnel wall. It was so located that its flow field did not interfere with the two probes in the center of the tunnel.

During the investigation the outrigger probe and the wall-mounted probe were used as free-stream Mach number calibration devices between the centerline of the test section and the wall. Continuous measurements of Mach number were obtained from the wall-mounted pitot-static probe for each test condition. Since there was a slight variation in Mach number across the test section, the Mach number determined from the pressure measurements obtained near the wall were corrected to the value at the experimental probe location. The correction was found by periodically traversing the outrigger probe to the center of the test section, which was the data acquisition location of the experimental probe. The difference between the Mach numbers found at the two locations was used to correct the Mach number value determined at the wall.

This procedure, however, accounts only for the variations in free-stream Mach number between the center of the test section and the wall. It does not account for possible variations in Mach number in the region of the test section covered during an angle of attack sweep. To vary angle of attack and angle of sideslip during a test run, the experimental probe and its support were mounted in a pitching mechanism that was mounted in the permanent strut of the wind tunnel. Since the pivot point of the pitching mechanism was not at the location of the experimental probe, the location of the probe in the test section varied considerably during an angle of attack sweep. However, when angle of sideslip alone was varied, the experimental probe remained in approximately the same position in the test section. It is believed that any variations in Mach number due to these effects did not significantly affect the results obtained.

INSTRUMENTATION AND ACCURACY

Figure 5 shows the locations of the internal static pressure orifices for probe tips 1, 2, 3, 4, and 5. The 300-series orifices, which were between 0.635 centimeter (0.25 inch) and 0.76 centimeter (0.30 inch) in back of the probe tip, were closest to the leading edge of the tips in all cases. The 100-series orifices were farther downstream inside the probe.

Also shown is the distance traveled by the internal total pressure tube. For tips 1, 2, and 5, the front end of the tube could be moved from a position at the downstream end of the 100-series orifices to a position outside the probe. For tips 3 and 4 the most upstream position of the tube was inside the probe.

The wind tunnel settling chamber pressure and the pressures for the pitot-static probes were measured with precision mercury manometers, which had an error level of ± 0.005 N/cm^2 (± 0.007 psi). The pressure inside the experimental probe's total pressure tube was measured with a single ± 3.4-N/cm^2 (± 5.0-psi) differential pressure transducer, which had an error level of ± 0.013 N/cm^2 (± 0.019 psi). The experimental probe's internal static pressures were measured with ± 10.3-N/cm^2 (± 15.0-psi) differential pressure transducers, which had an error level of ± 0.022 N/cm^2 (± 0.032 psi). The free-stream Mach number of the test section's centerline was determined from pitot-static pressure measurements and was accurate to ± 0.005. Local Mach numbers at the experimental probe were determined from

measurements made at the internal static pressure orifices and total pressure tube and was accurate to ±0.01.

Angle of attack was measured by using an accelerometer angular position transducer, which had an error of ±0.02°. Angle of sideslip was measured with a variable resistance angular position transducer, which had an error of ±0.1°. Since flow angularity in the test section was not determined for these tests, the accuracy of the angle of attack and angle of sideslip of the wind tunnel airflow cannot be given.

RESULTS AND DISCUSSION

All the tips tested exhibited similar characteristics. The probe bow shock was swallowed and kept within the probe throughout the angle of attack and angle of sideslip ranges tested. The effects of changing the position of the total pressure tube and sleeve were similar for all the tips tested. Therefore, the results are discussed in detail for tip 1 only; the discussion of the other tips is brief.

Tip 1

Effect of sleeve position and internal total pressure tube position. – Figure 6 shows Schlieren photographs of both the swallowed and the expelled bow shock. In figure 6(a), which was taken while the shock was swallowed, the sleeve is in the wide-open position and a portion of the complex internal shock pattern appears through the openings. In figure 6(b) the sleeve is in the closed position and the bow shock is expelled.

The effect of opening the sleeve on Mach number error, ΔM, is shown in figure 7. Local Mach number was calculated from total pressure and the average of the static pressures obtained from static pressure orifices 303 and 307. Two regimes of probe operation are indicated – shock expelled and shock swallowed. When the shock is expelled, the Mach number error is unacceptably large; when the shock is swallowed, the error is low and averages approximately -0.03. Once the shock is swallowed, which occurs when the sleeve is approximately 25 percent open, ΔM is unaffected by further increases in exit opening. The test Mach number error for the point just before the shock is swallowed agrees closely with the theoretical Mach number error for shock-expelled operation when the normal shock is at the tip entrance.

Figure 8 shows the effect of the position of the internal total pressure tube on the total pressure ratio, p_{t_i}/p_{t_∞}, for several angles of attack. The sleeve was wide open for the tests. For positions near the probe tip, both inside and outside the test probe, there is no difference between indicated total pressure and free-stream total pressure. However, as the tube moves downstream in the probe, internal shock wave effects become evident. Similarly, figure 9 shows the effect of total pressure tube position on Mach number error. Local Mach number error was calculated from total pressure and the average of the static pressures obtained from static

pressure orifices 303 and 307. The effects of internal shock waves are evident in the data farther upstream than in the total pressure data in figure 8. The minimum Mach number error excluding the shock wave region ranges from 0.025 to 0.050 and occurs when the tube is near the probe tip.

Effect of angle of attack and angle of sideslip.– Figure 10 shows the Mach number errors for individual static pressure orifices as a function of angle of attack. Angle of sideslip was approximately 0°. The 300-series orifices (fig. 10(a)) show linear variation over a reasonably wide range of angle of attack. Of the orifices shown, orifices 303 and 307 are the least affected by changes in angle of attack and show the lowest values of ΔM. The 100-series orifices (fig. 10(b)) exhibit nonlinear variation throughout the angle of attack range. The nonlinearities indicate strong internal shock wave effects, and Mach number error increases as angle of attack changes positively or negatively from 0°. Consequently, data from these orifices for all tips were eliminated in further data analysis.

Figures 11(a) to 11(c) show the variation of Mach number error with angle of sideslip for fixed angles of attack of approximately 0°, 3°, and 5°, respectively. Quasi-linear relations are evident for all of the 300-series orifices. Static pressure orifices 303 and 307 show essentially the same variation with sideslip for all three angles of attack. The variation of the other orifices for the three angles of attack differs, however.

Since the pressures from orifices 303 and 307 were affected least by changes in angle of attack (figs. 10 and 11), they were used in further Mach number error analysis. Figure 12(a) shows the Mach number error obtained by averaging the static pressures measured at orifices 303 and 307 versus angle of attack. Data for two Reynolds numbers are shown, and the higher Reynolds number data show a lower ΔM than the lower Reynolds number data. Data from three conventional probes are also shown. At the low angles of attack for which comparisons are possible, the shock-swallowing probe results are comparable to the results for the conventional probes.

Figure 12(b) shows the variation of Mach number error for the average of the pressures from orifices 303 and 307 with angle of sideslip. Data are shown for two Reynolds numbers for an angle of attack of approximately 0° and also for approximate angles of attack of 0°, 3°, and 5° for one Reynolds number. These data also show a lower ΔM at the higher Reynolds number. Up to $\beta \approx \pm 2°$, ΔM varies little with angle of sideslip. Beyond $\beta \approx \pm 2°$, ΔM increases markedly. The effect of angle of attack on ΔM, which is shown on the right, is slight.

Figure 13 illustrates the use of the shock-swallowing probe to measure angle of attack by plotting the parameter $\dfrac{p_{301} - \dfrac{p_{307} + p_{303}}{2}}{p_{t_i}}$ versus angle of attack. This parameter shows a predictable relationship with angle of attack but is little affected by Reynolds number. The data are shown for an angle of sideslip of approximately 0°. Similarly, figure 14 shows the use of the shock-swallowing probe to measure

angle of sideslip by plotting the parameter $\frac{p_{307} - p_{303}}{p_{t_i}}$ against angle of sideslip. The parameter shows excellent linearity with angle of sideslip for the test conditions and is not affected by Reynolds number or angle of attack.

Tips 2, 3, 4, and 5

Figure 15 and 16 present ΔM versus angle of attack and angle of sideslip, respectively, for tip 2. These data closely resemble the corresponding data for tip 1 (figs. 10 and 11) except for the abrupt change in ΔM in figure 15 at $\alpha \approx 13°$. This change does not occur in the tip 1 angle of attack data.

Figure 17 shows ΔM versus angle of attack for tip 3 with orifices 301 and 307 oriented in the horizontal plane. These results are generally inferior to the corresponding results for tips 1 and 2 in that there are large Mach number errors for all the orifices.

Figures 18 and 19 present ΔM versus angle of attack and angle of sideslip, respectively, for tip 4. The data were obtained with orifices 303 and 307 oriented in the horizontal plane. In figure 18, there are low Mach number errors for orifices 301, 302, 303, 307, 308, and 309 throughout the angle of attack range. In figure 19, these orifices behave like orifices 303 and 307 in tips 1 and 2.

Figures 20 and 21 present ΔM versus angle of attack and angle of sideslip, respectively, for tip 5. In figure 20, the data resemble the corresponding data for tips 1 and 2 except at $\alpha > 7°$. The data in figure 21 closely resemble the corresponding data for tips 1 and 2.

In general, the results from tips 2, 4, and 5 are roughly comparable to the results from tip 1, whereas the results from tip 3 are inferior.

CONCLUSIONS

A brief wind tunnel test was conducted at a Mach number of 1.83 to explore the feasibility of using a shock-swallowing airspeed probe for high-speed aircraft. Tests were conducted over an approximate angle of attack range from -5° to 15° and an approximate angle of sideslip range of ±4° and for various probe tip shapes. Reynolds number ranged from approximately 8.2×10^6 per meter (2.5×10^6 per foot) to approximately 16.4×10^6 per meter (5×10^6 per foot). The following conclusions were drawn:

For all probe tips tested, the bow shock was swallowed and kept within the probe over the test angle of attack and angle of sideslip ranges.

There was no difference between the total pressure measured by the movable internal total pressure tube and free-stream total pressure when the tube was near the probe tip. Mach number error was also at a minimum when the total pressure tube was close to the probe tip.

Once the exit area was opened far enough to permit the shock to be swallowed, Mach number error was insensitive to further increases in exit area. The Mach number error before the shock was swallowed agreed closely with theoretical predictions of Mach number error for shock-expelled operation with the normal shock at the probe entrance.

For four of the five tips tested, the Mach number error derived by averaging two static pressures measured at horizontally opposed positions near the probe entrance was least sensitive to angle of attack. The Mach number error so derived was comparable to the errors obtained for conventionally designed airspeed sensors. The same orifices were used to derive parameters that gave indications of angle of attack and angle of sideslip.

The results from four of the five tips tested were roughly comparable. The results from a fifth were generally inferior.

For all tips, the static orifices on the internal wall close to the probe tip produced the best data, because the orifices farther downstream were affected by internal shock waves and generally produced erratic results.

Flight Research Center
National Aeronautics and Space Administration
Edwards, Calif., March 10, 1975

REFERENCES

1. Webb, Lannie D.: Characteristics and Use of X-15 Air-Data Sensors. NASA TN D-4597, 1968.

2. Webb, Lannie D.; and Washington, Harold P.: Flight Calibration of Compensated and Uncompensated Pitot-Static Airspeed Probes and Application of the Probes to Supersonic Cruise Vehicles. NASA TN D-6827, 1972.

3. Penland, Jim A.; Creel, Theodore R., Jr.; and Howard, Floyd G.: Experimental Low-Speed and Calculated High-Speed Aerodynamic Characteristics of a Hypersonic Research Airplane Concept Having a 65° Swept Delta Wing. NASA TN D-7633, 1974.

4. Krause, Lloyd N.; and Glawe, George E.: Performance of a Mass-Flux Probe in a Mach 3 Stream. NASA TN D-5563, 1969.

5. Rose, R. E.: The Shock Adjustment Concept — A New Method for Improved Supersonic Air Data Sensing. Flight Testing Today — 1973, Proceedings of the Fourth National Symposium, Soc. Flight Test Eng., 1973.

6. Richardson, Norman R.; and Pearson, Albin O.: Wind-Tunnel Calibrations of a Combined Pitot-Static Tube, Vane-Type Flow-Direction Transmitter, and Stagnation-Temperature Element at Mach Numbers From 0.60 to 2.87. NASA TN D-122, 1959.

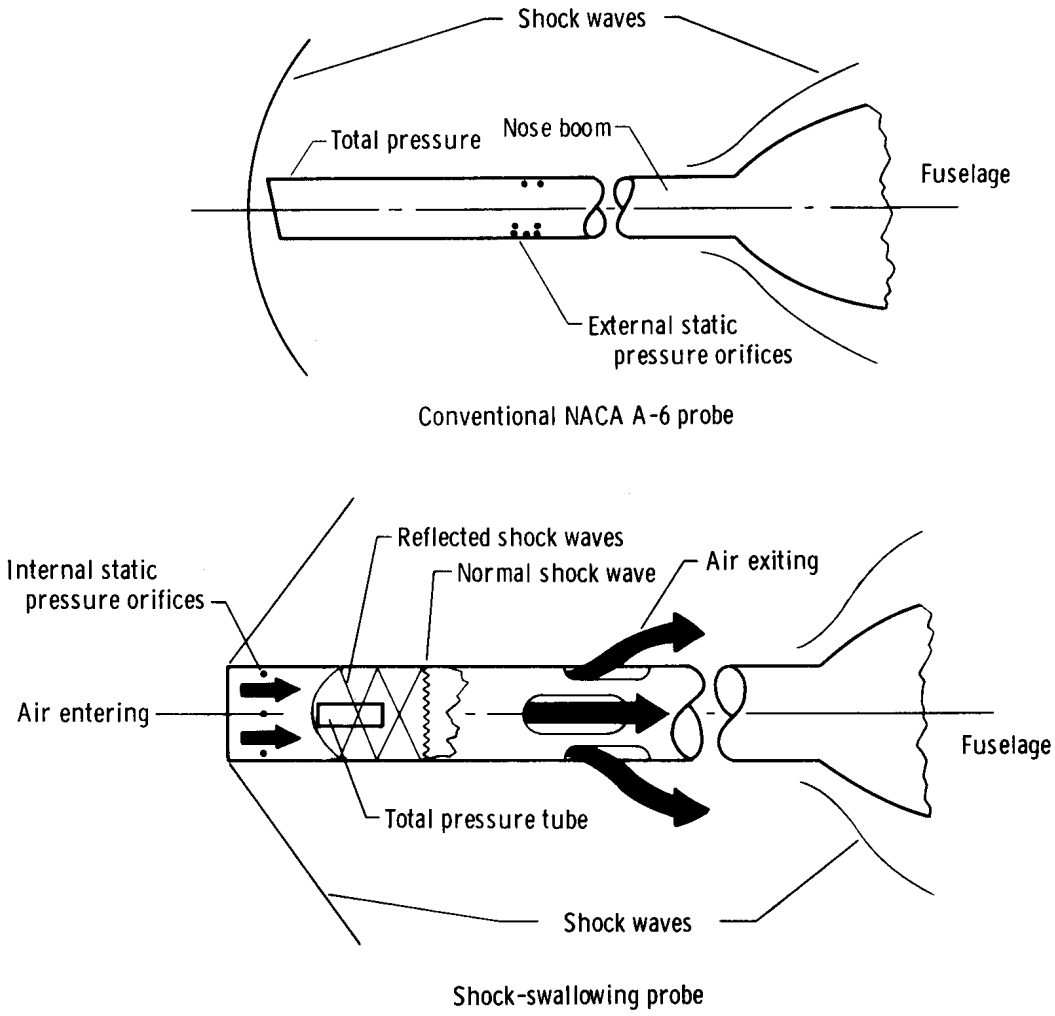

Figure 1. Operation of a shock-swallowing airspeed probe and a conventional airspeed probe at supersonic speeds.

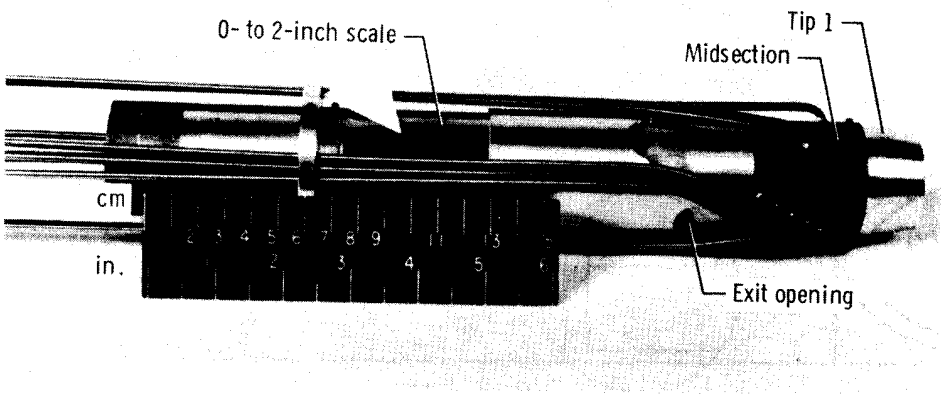

E-19657

(a) Minimum exit opening.

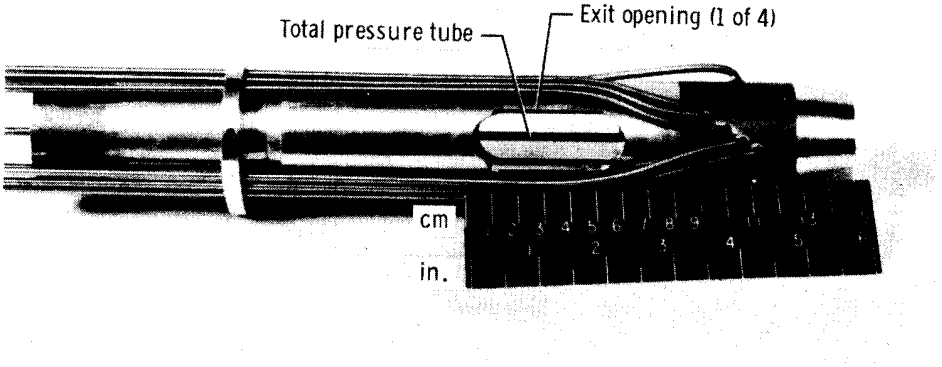

E-19658

(b) Maximum exit opening.

Figure 2. Wind tunnel test probe with minimum and maximum openings in external sleeve.

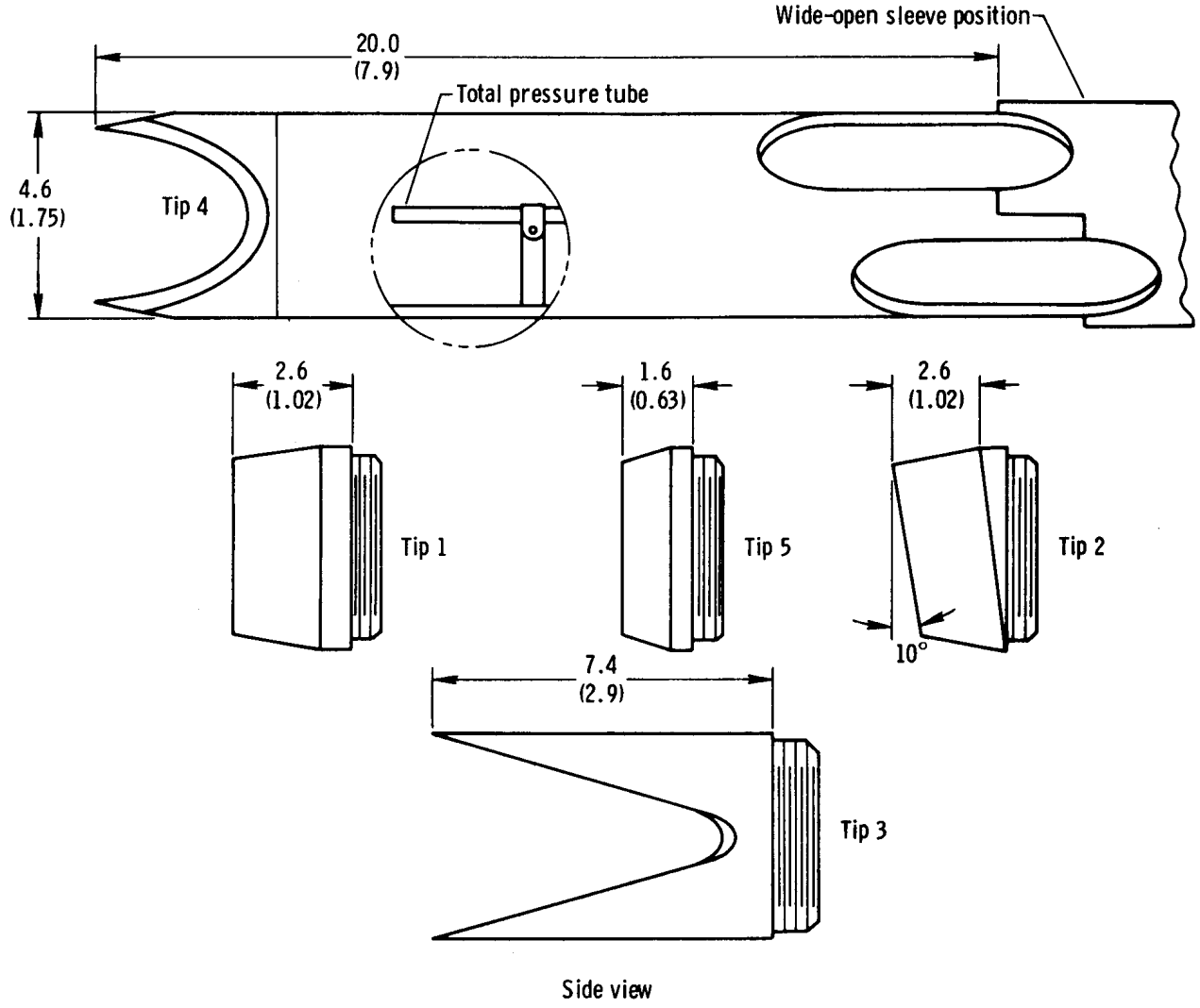

Figure 3. Pitot-static probe with interchangeable tips, movable sleeve, and movable total pressure tube. Dimensions in centimeters (inches).

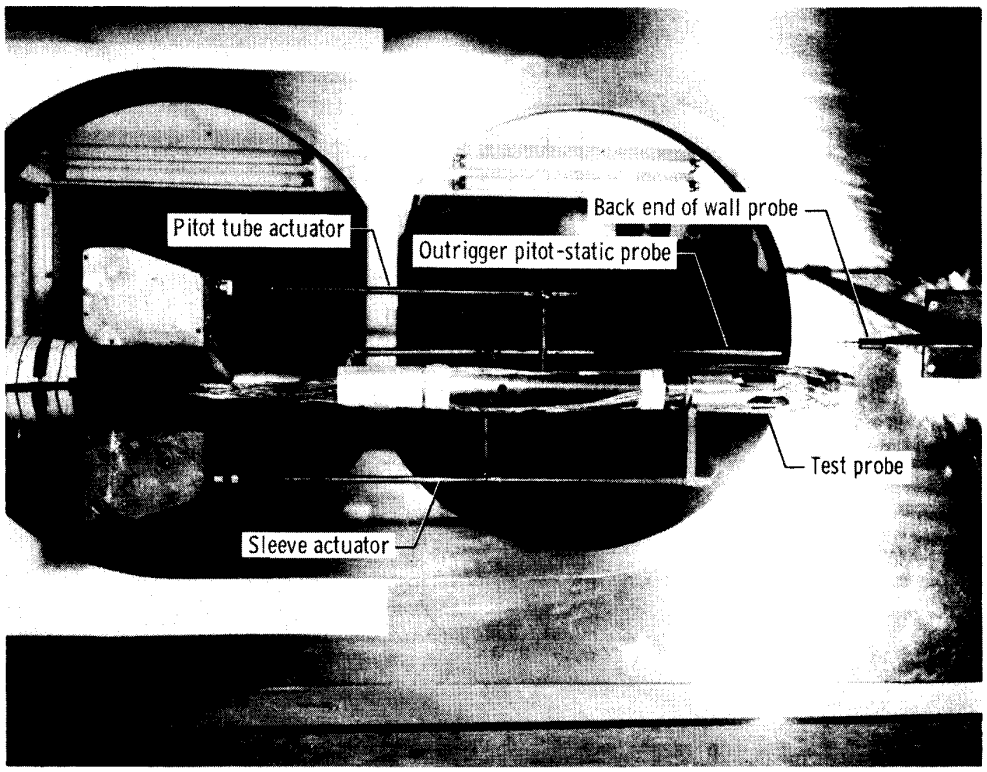

Figure 4. Probe mounted in wind tunnel.

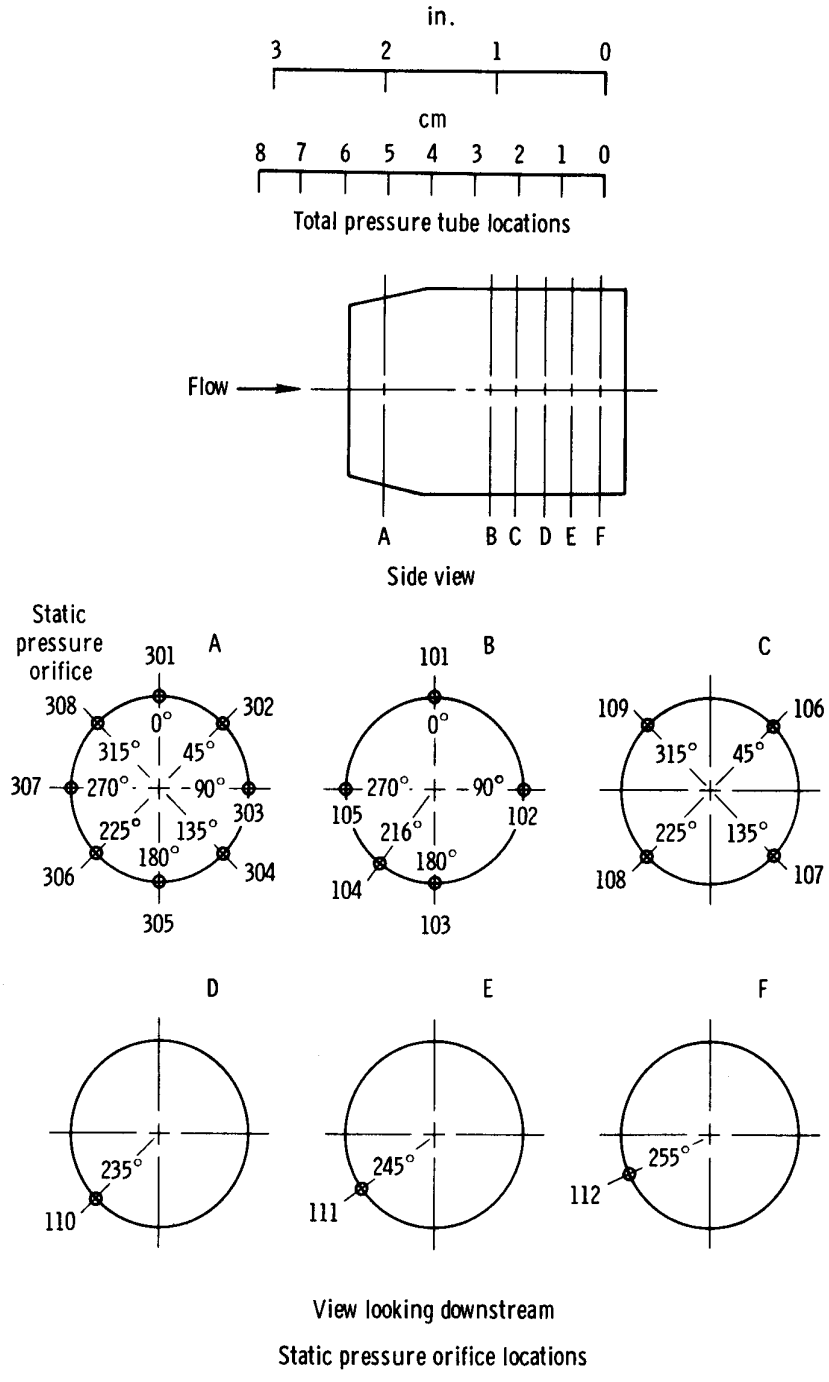

(a) Tip 1.

Figure 5. Total pressure and static pressure orifice locations for probes tested. Total pressure tube and static pressure orifices are internal.

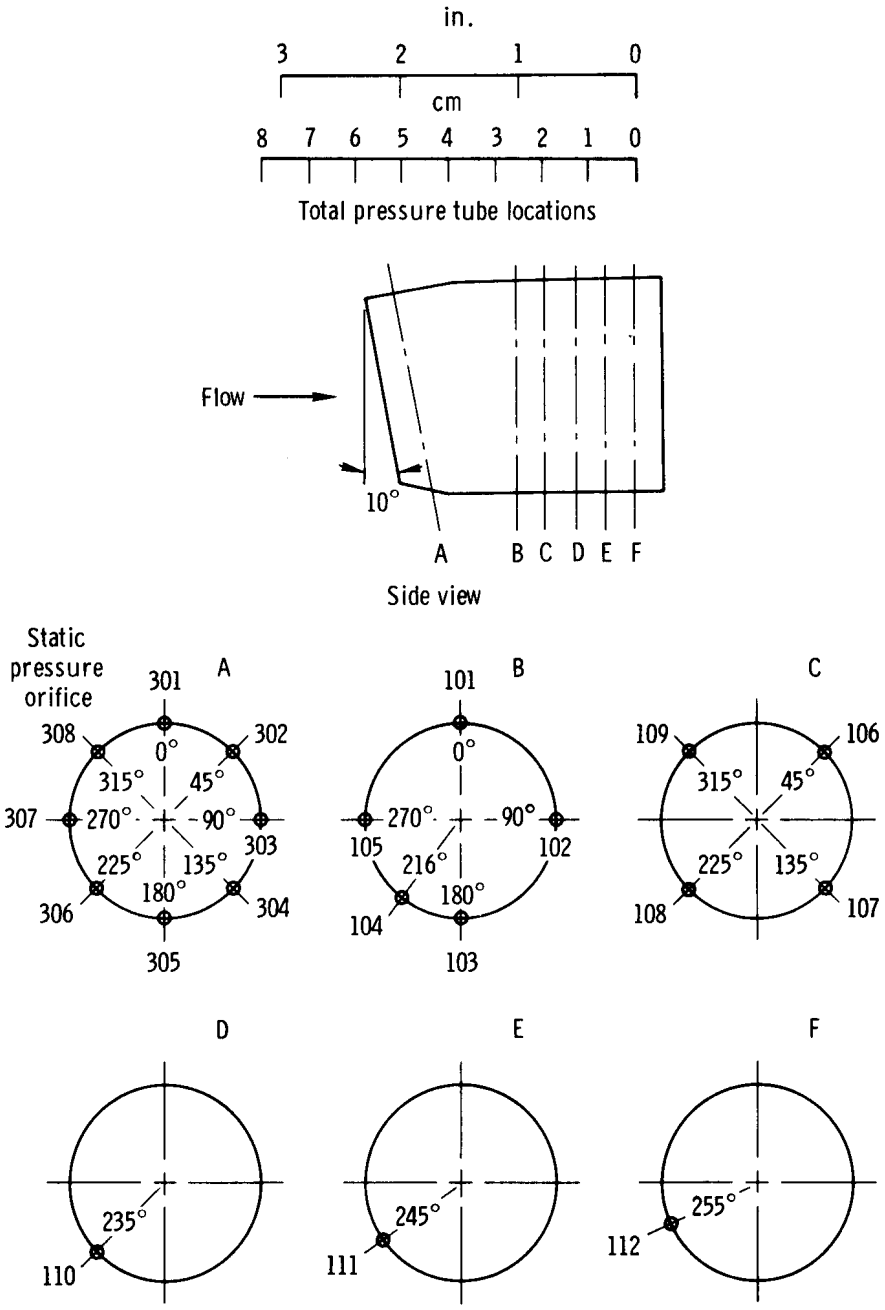

(b) Tip 2.

Figure 5. Continued.

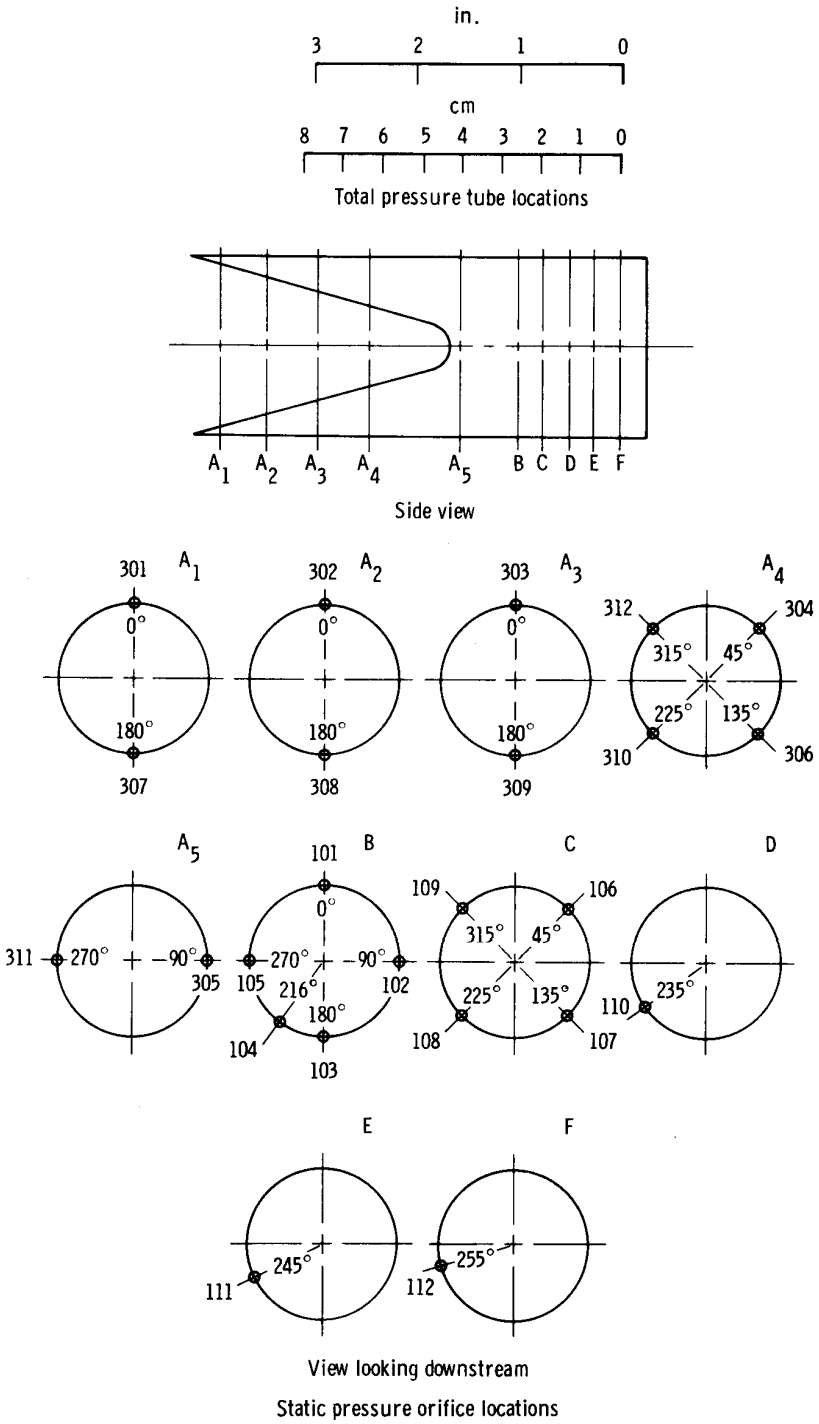

(c) Tip 3.

Figure 5. Continued.

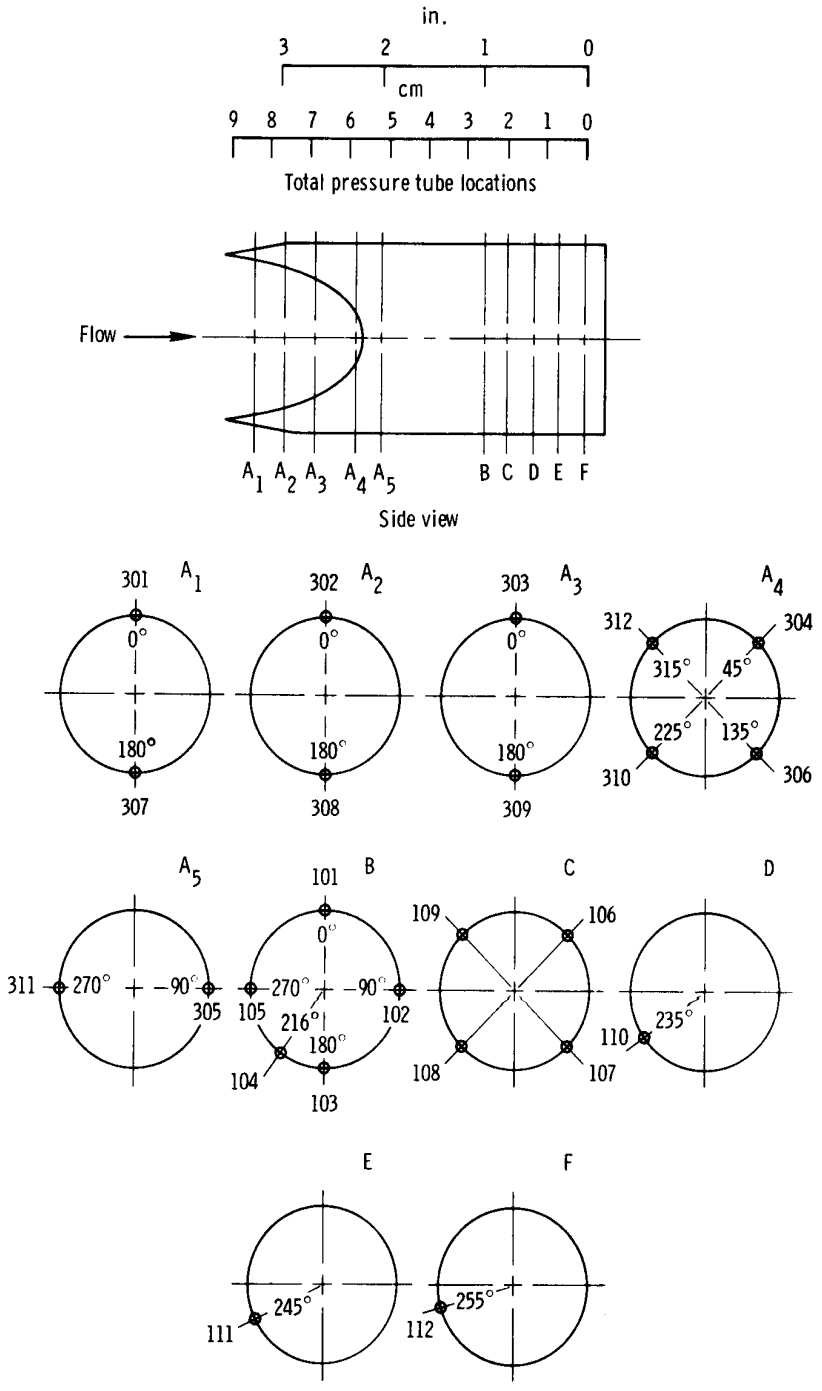

(d) Tip 4.

Figure 5. Continued.

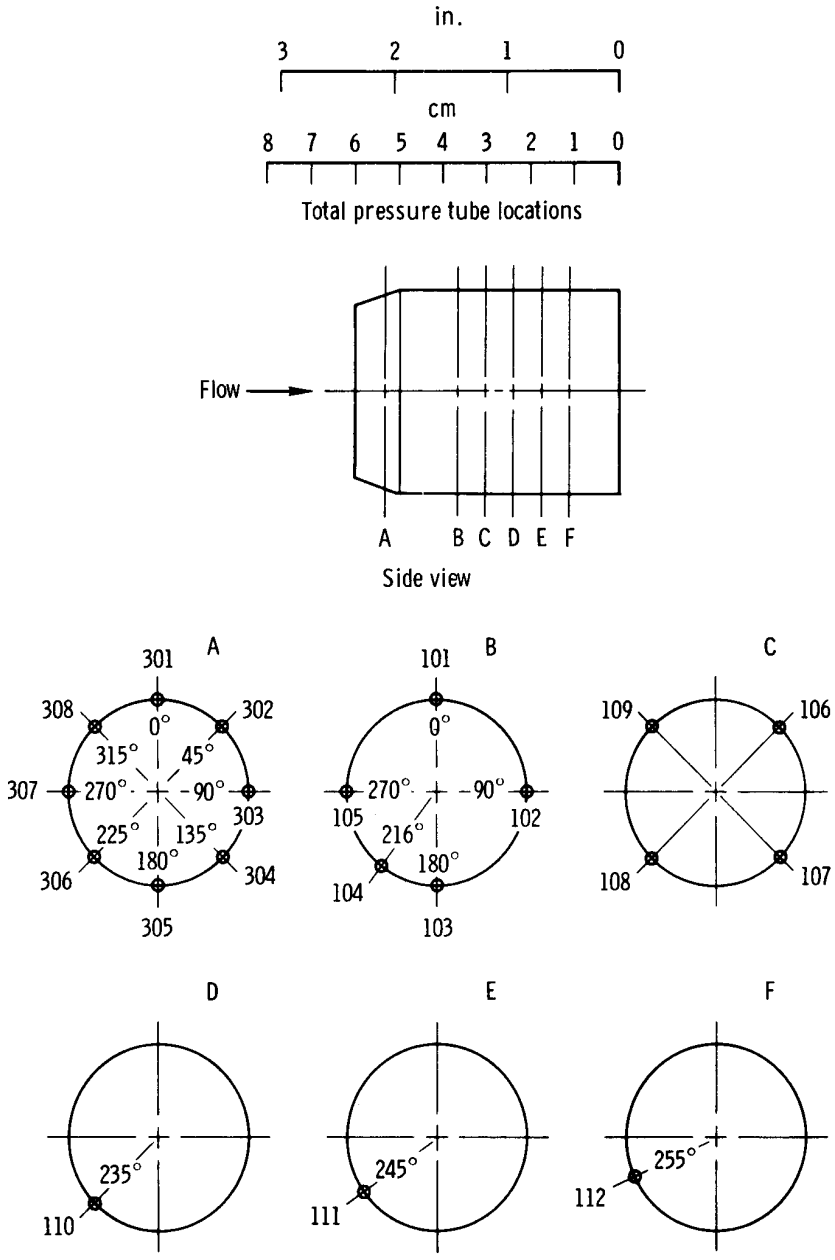

(e) Tip 5.

Figure 5. Concluded.

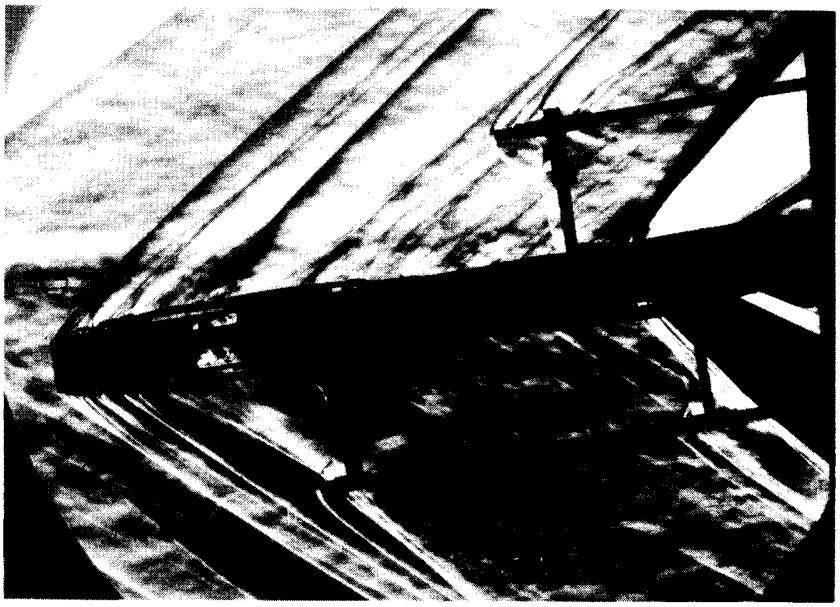

(a) Shock swallowed.

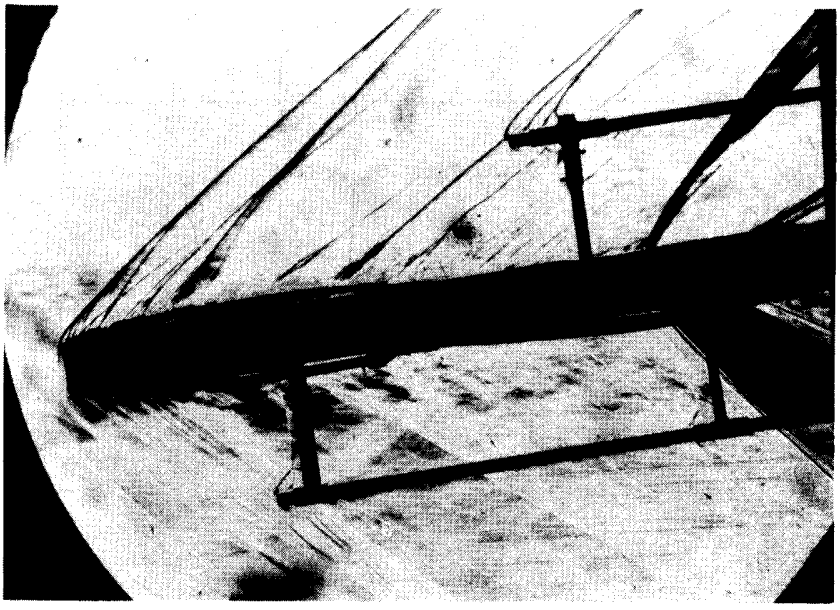

(b) Shock expelled.

Figure 6. Schlieren photographs of probe swallowing and expelling shock.

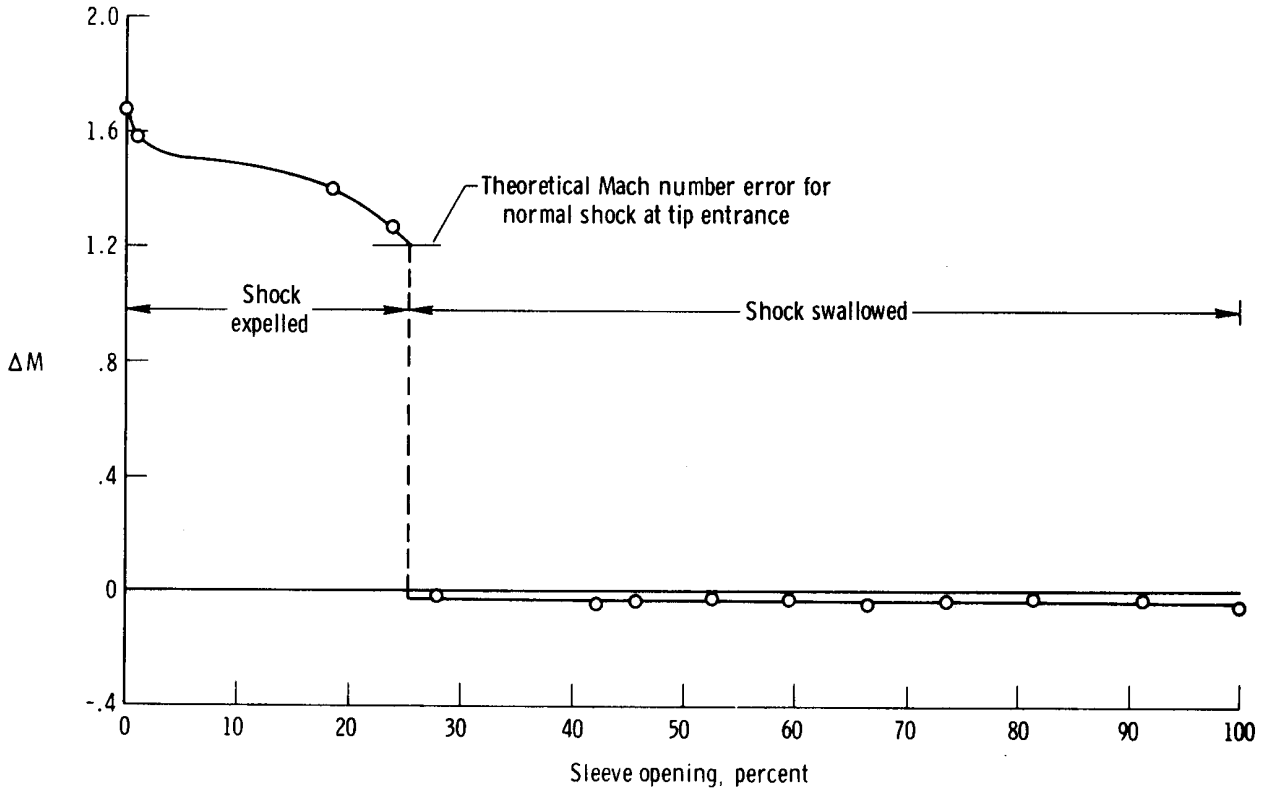

Figure 7. Effect of amount of sleeve opening on Mach number error for tip 1. $M \approx 1.83$; $\alpha \approx 0°$.

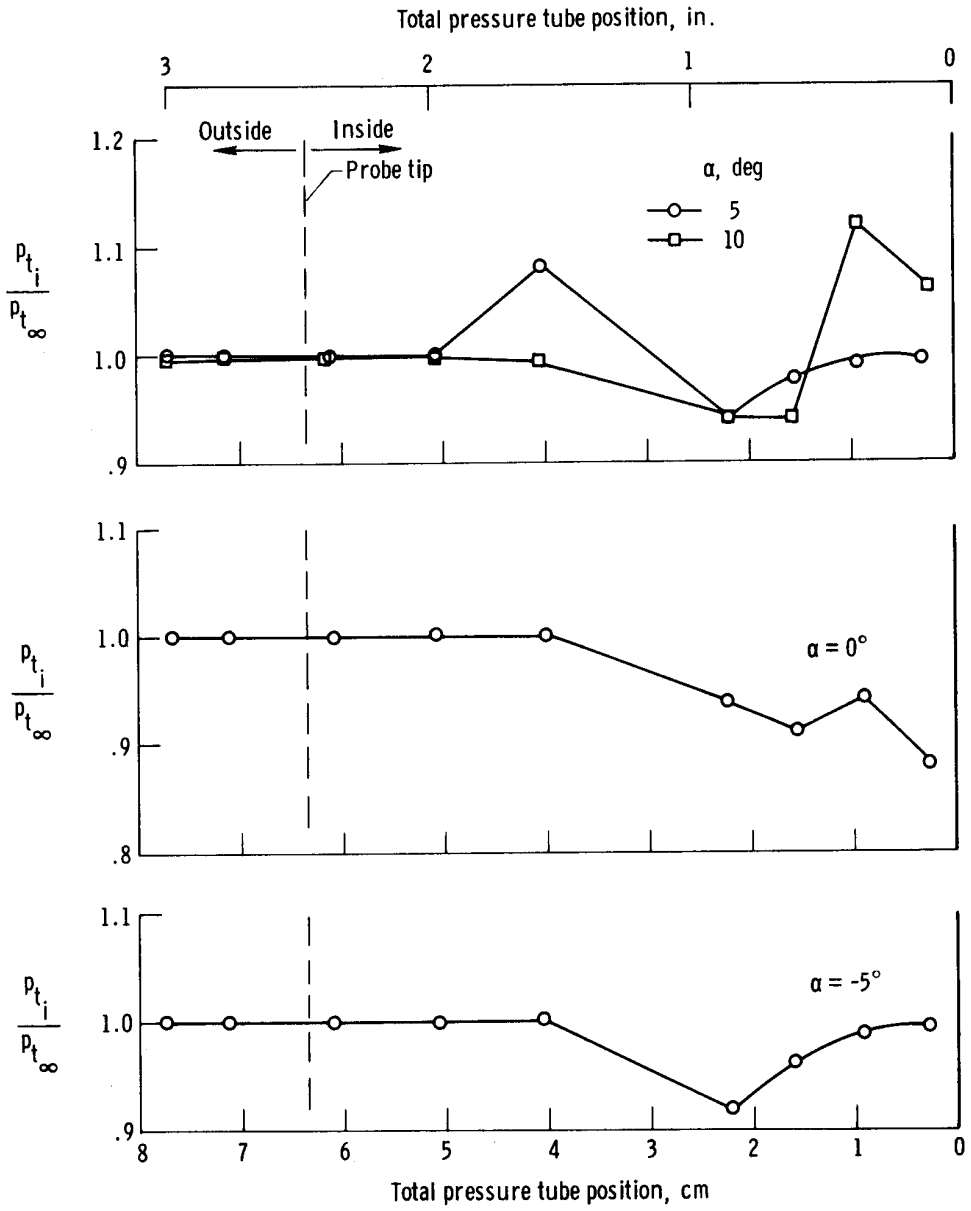

Figure 8. Effect of internal total pressure tube position on total pressure ratio for tip 1. Sleeve wide open; shock swallowed; $M \approx 1.83$.

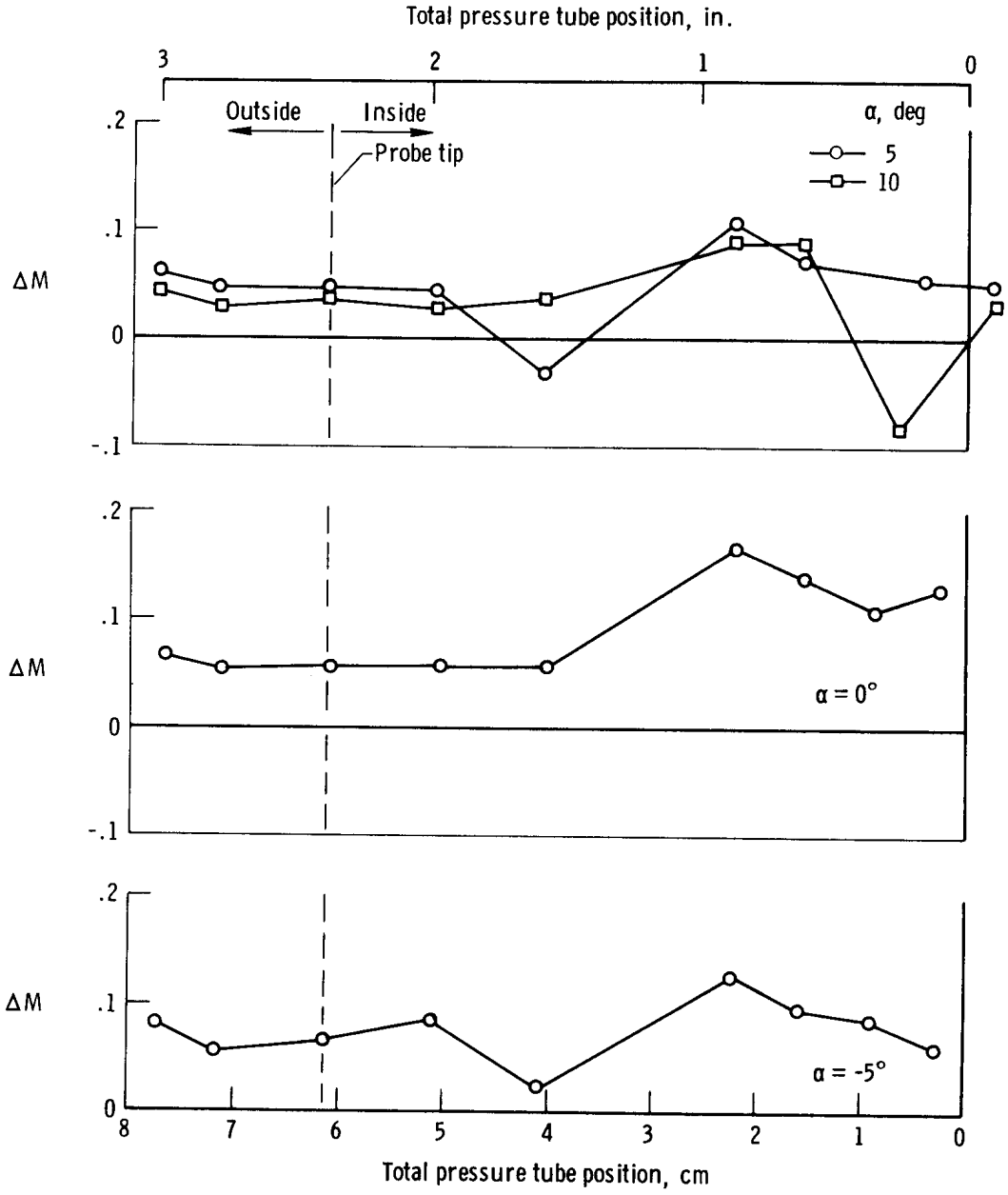

Figure 9. Effect of internal total pressure tube position on Mach number error for tip 1. Sleeve wide open; shock swallowed; $M \approx 1.83$.

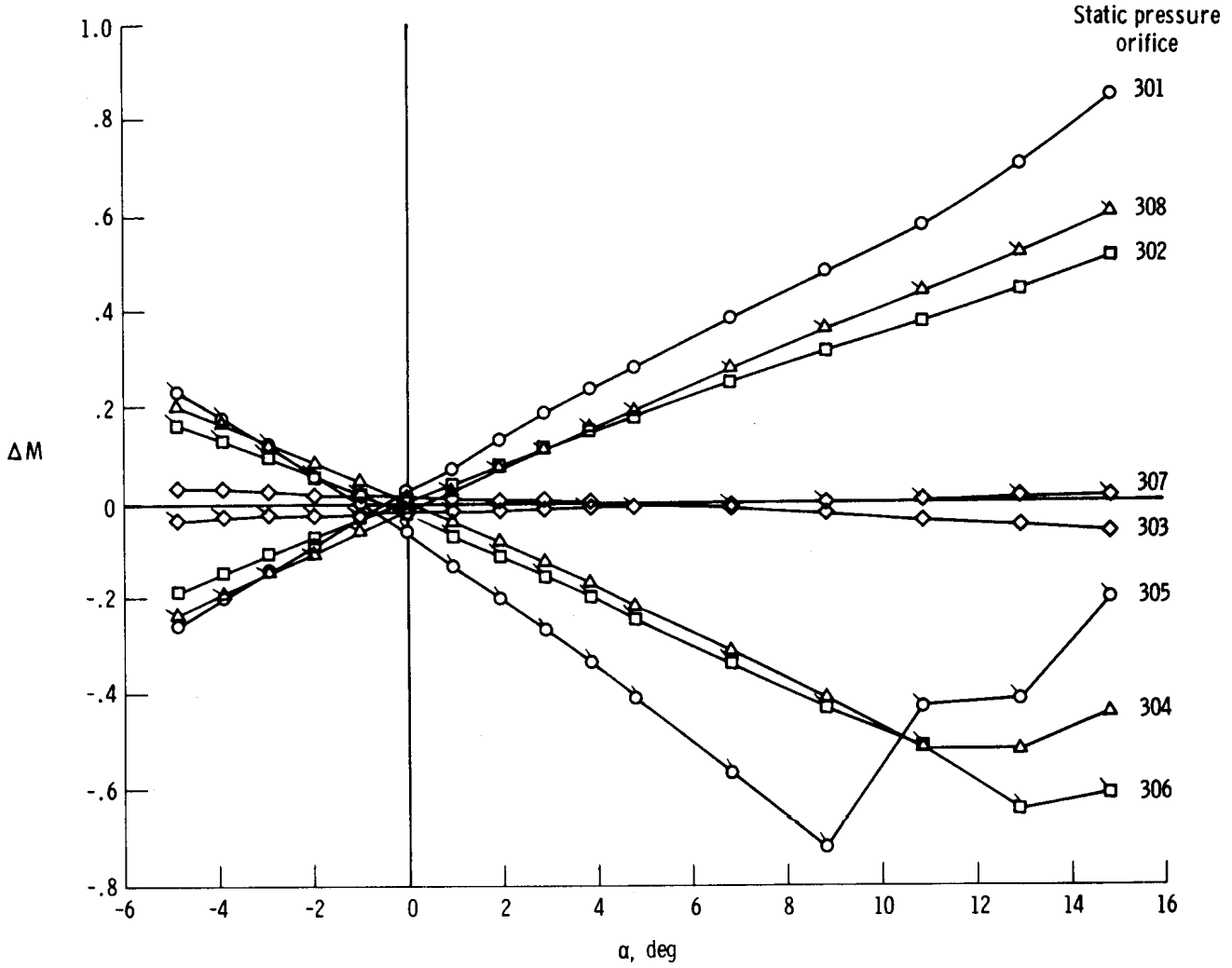

(a) 300-series orifices.

Figure 10. Mach number error versus angle of attack for tip 1. β ≈ 0°.

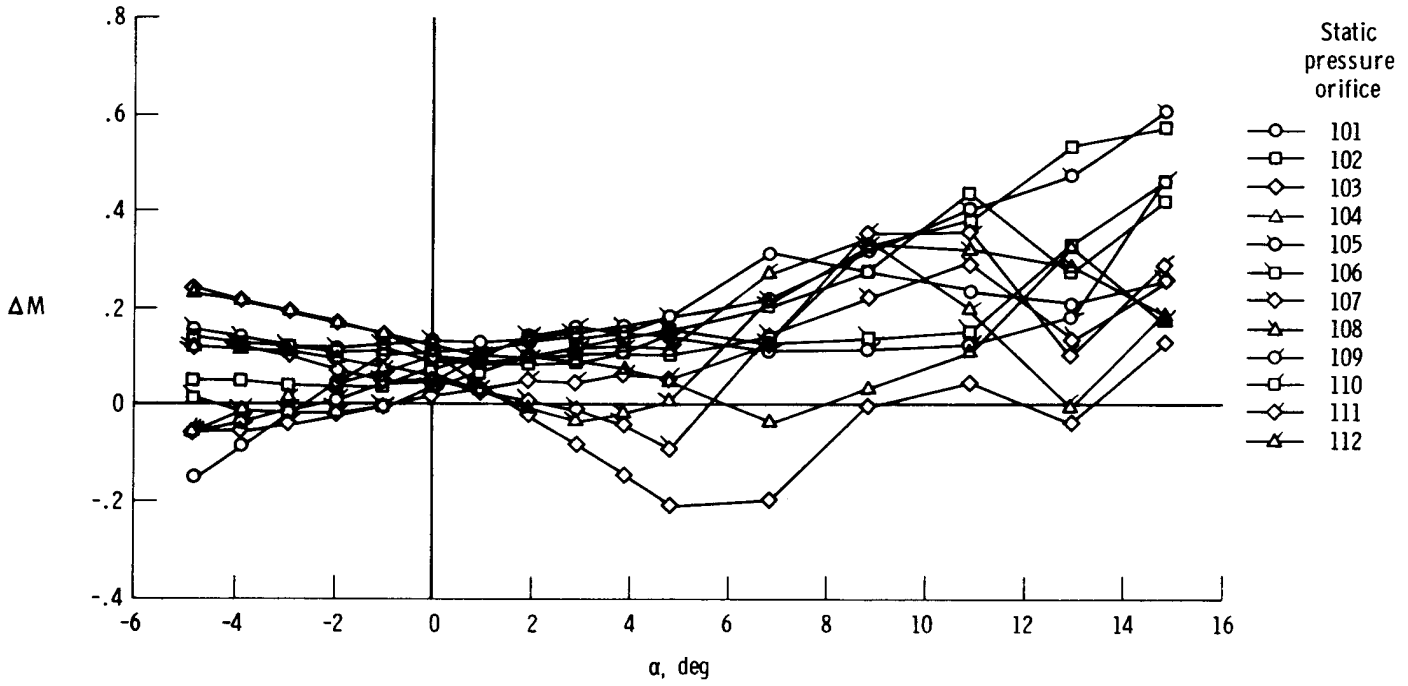

(b) 100-series orifices.

Figure 10. Concluded.

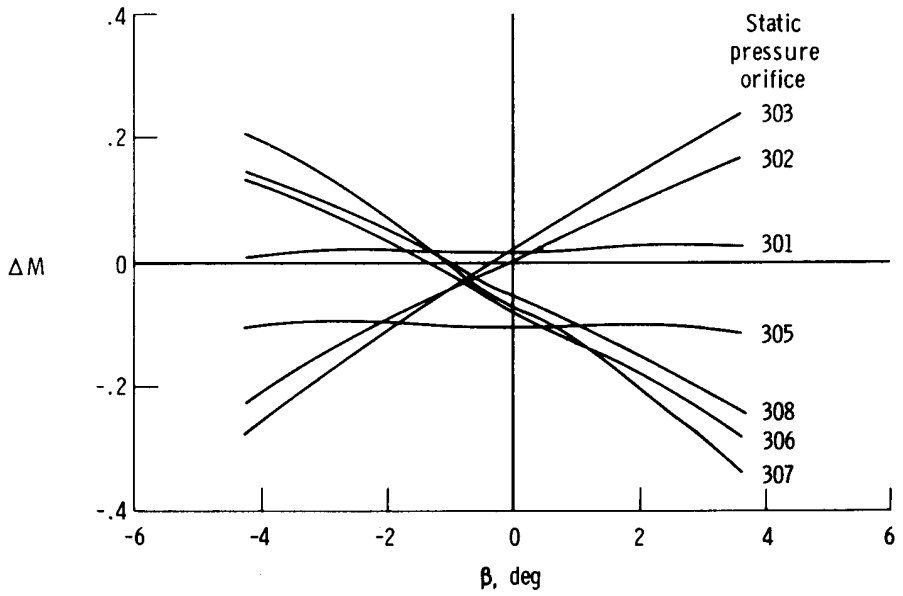

(a) $\alpha \approx 0°$.

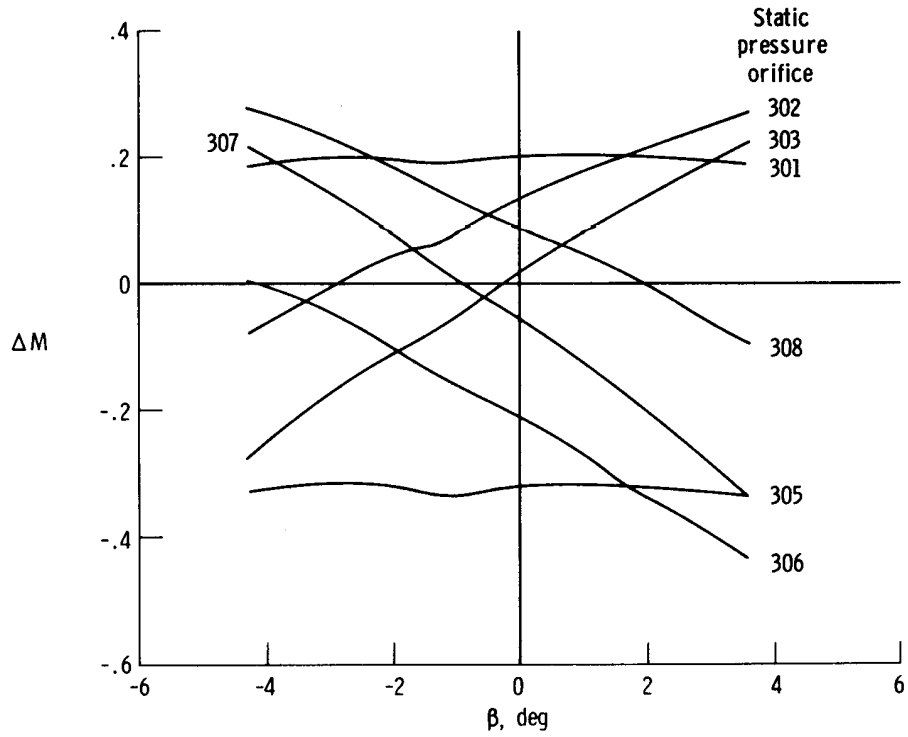

(b) $\alpha \approx 3°$.

Figure 11. Mach number error versus angle of sideslip for tip 1.

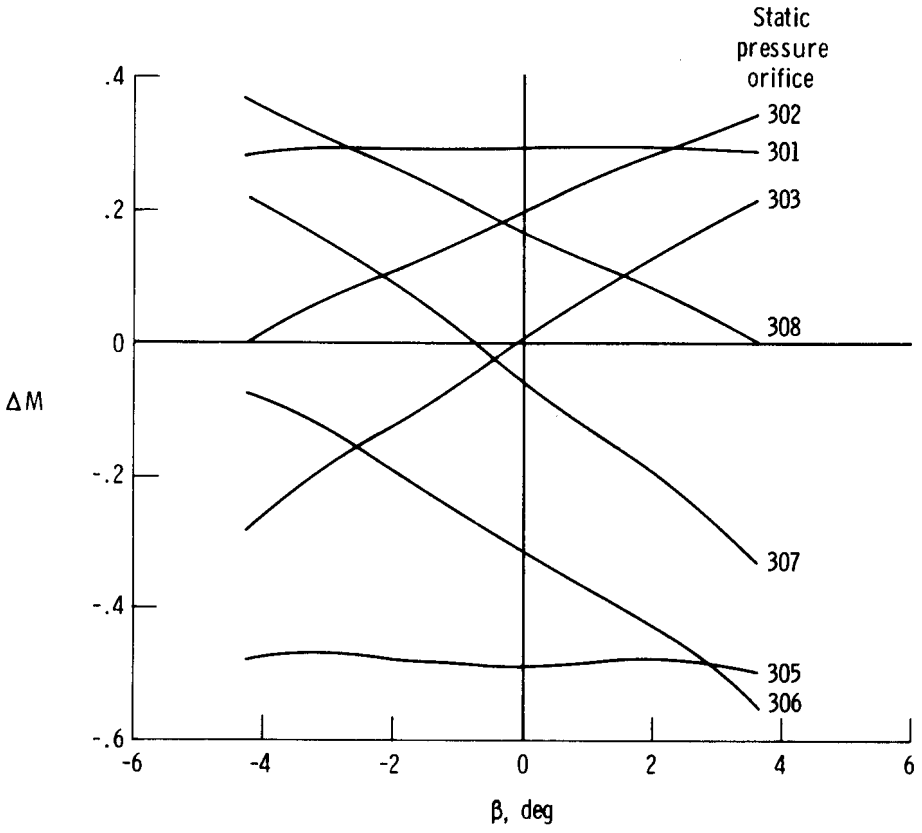

(c) $\alpha \approx 5°$.

Figure 11. Concluded.

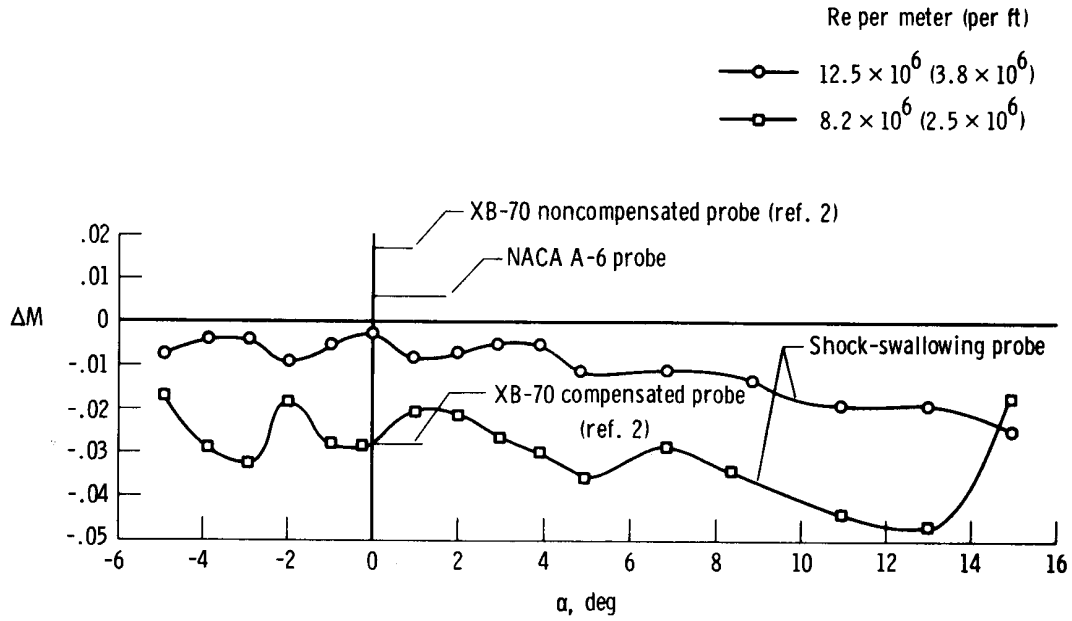

(a) Effect of angle of attack. β ≈ 0°.

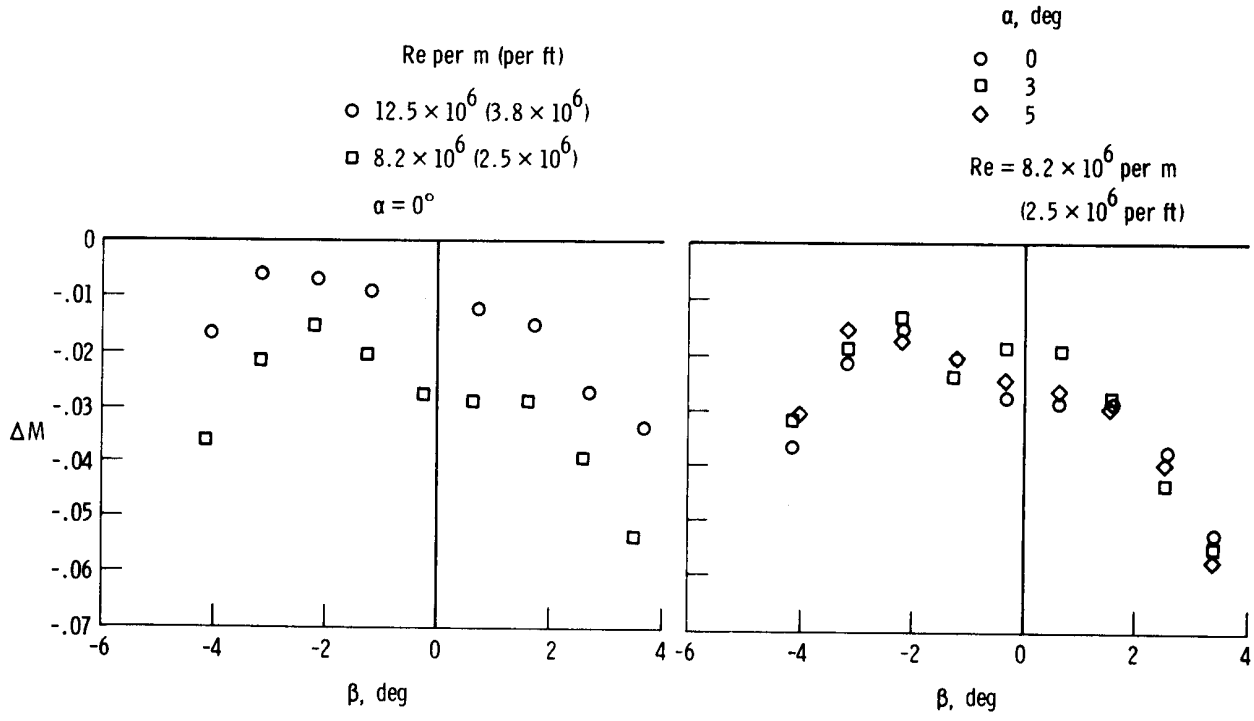

(b) Effect of angle of sideslip.

Figure 12. Mach number error resulting from average of static pressures measured at orifices 303 and 307. Tip 1.

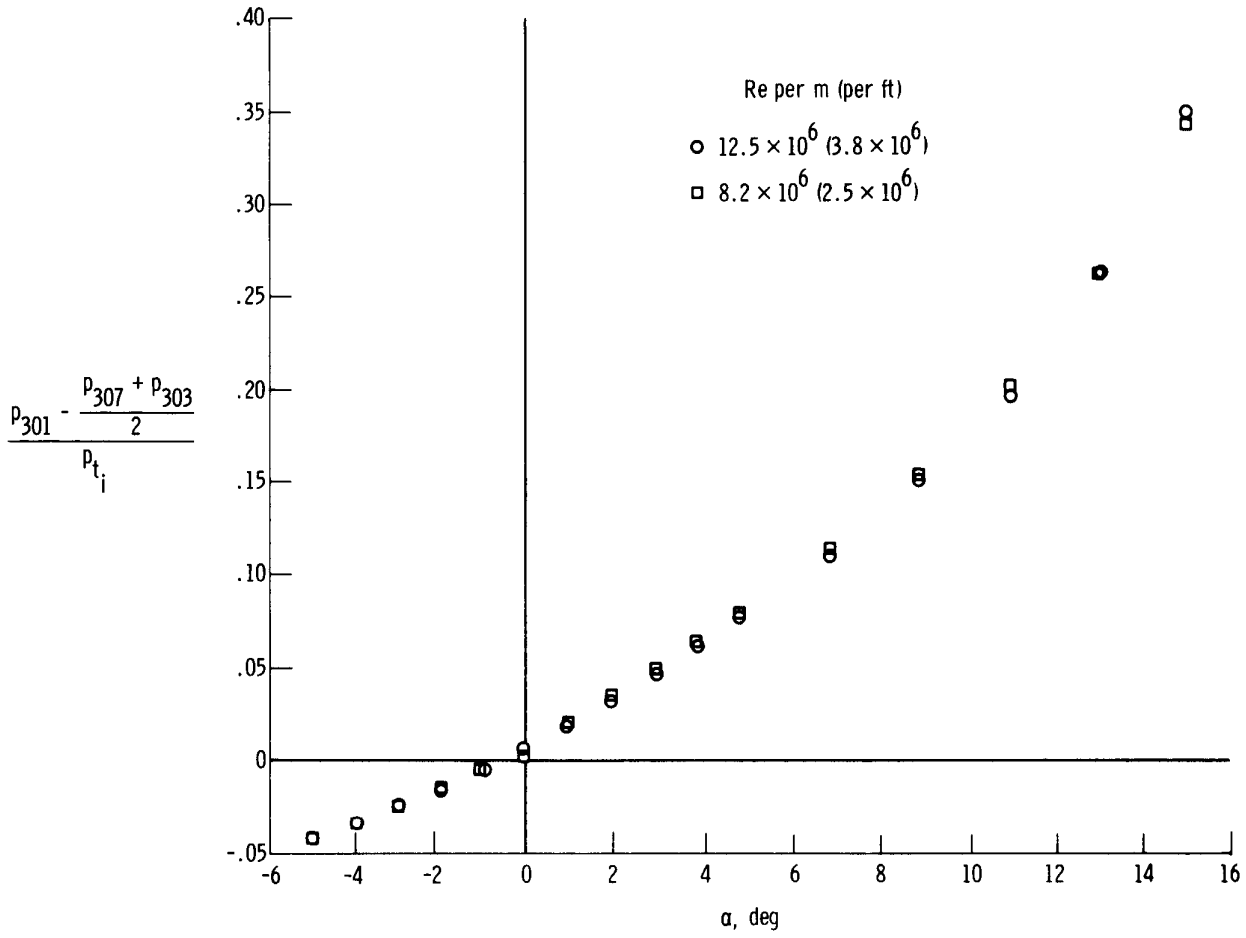

Figure 13. Calibration showing use of shock-swallowing probe to measure angle of attack. $\beta \approx 0°$, tip 1.

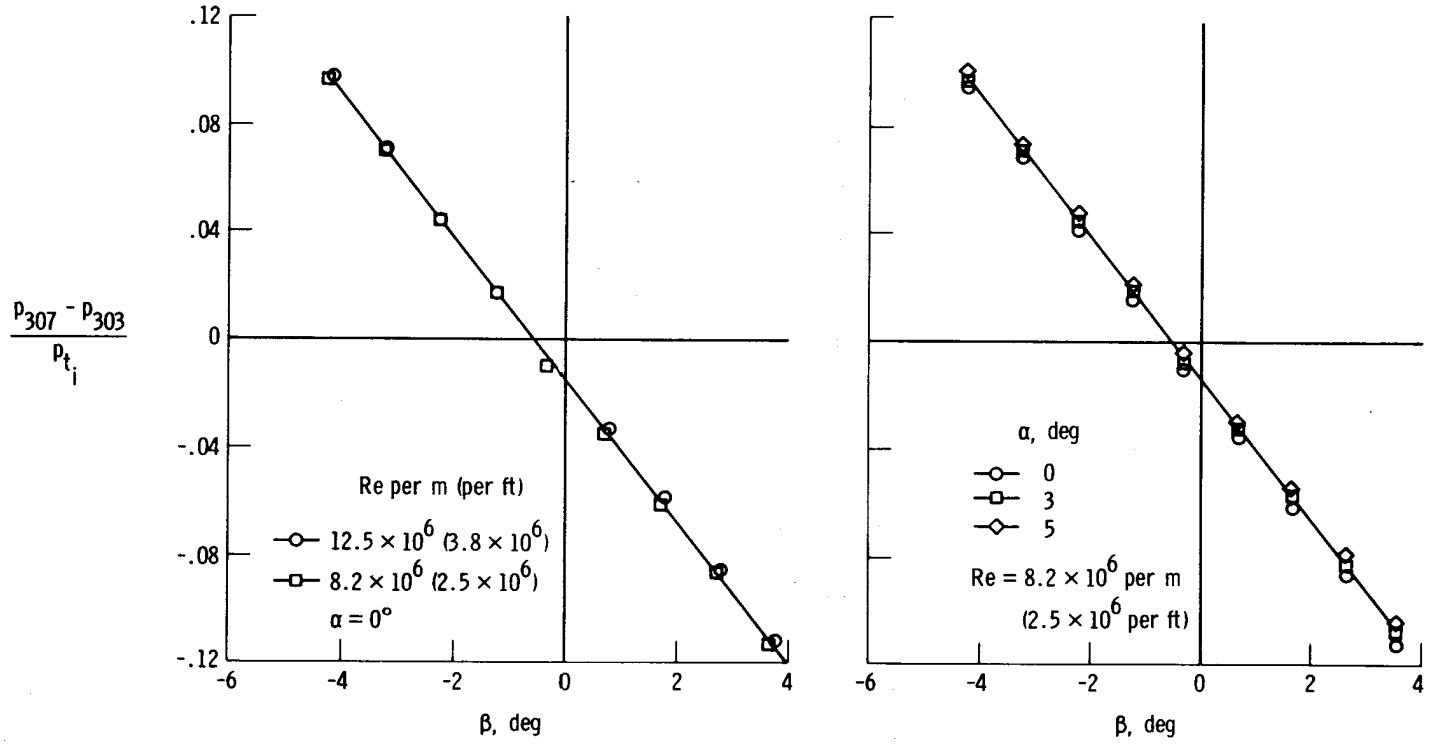

Figure 14. Calibration showing use of shock-swallowing probe to measure angle of sideslip. Tip 1.

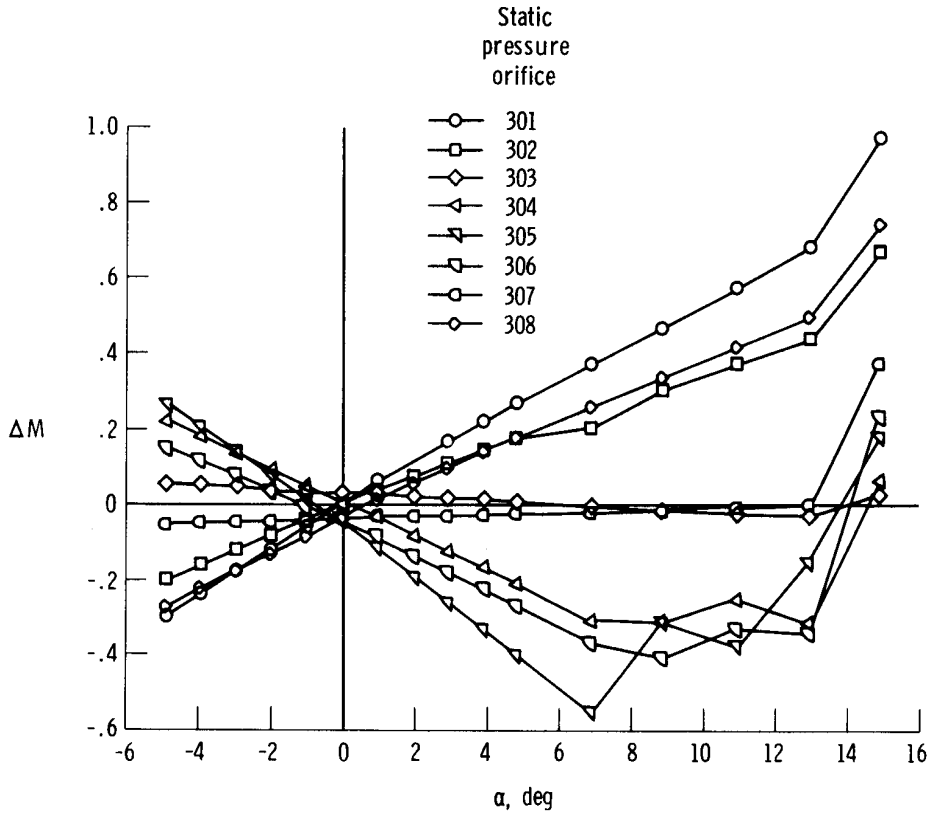

Figure 15. Mach number error versus angle of attack for the 300-series orifices in tip 2. Sleeve wide open; total pressure tube position = 5.1 cm (2.0 in.); Re ≈ 16.4 × 10^6 per m (5 × 10^6 per ft); β ≈ 0°.

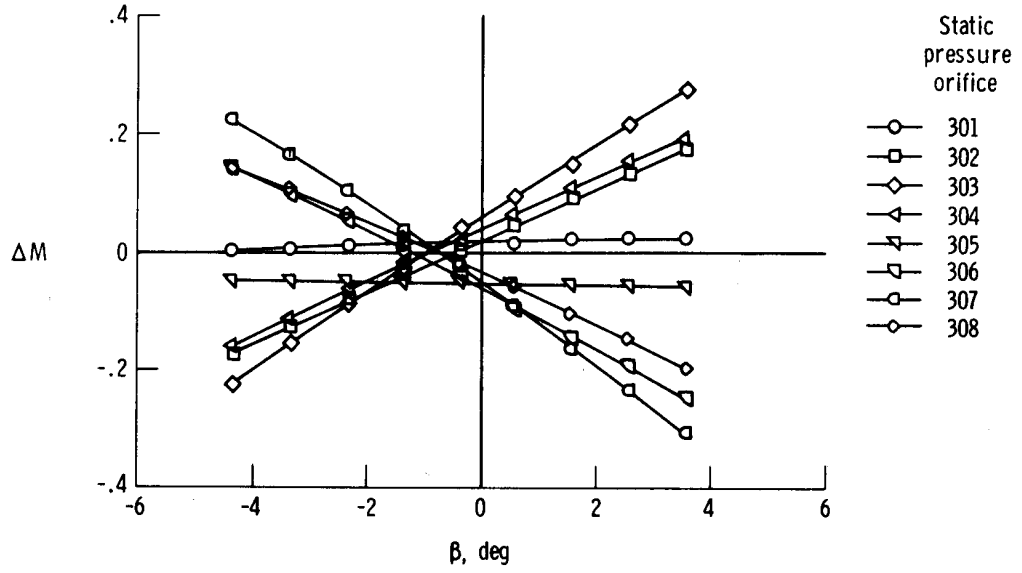

(a) $\alpha \approx 0°$.

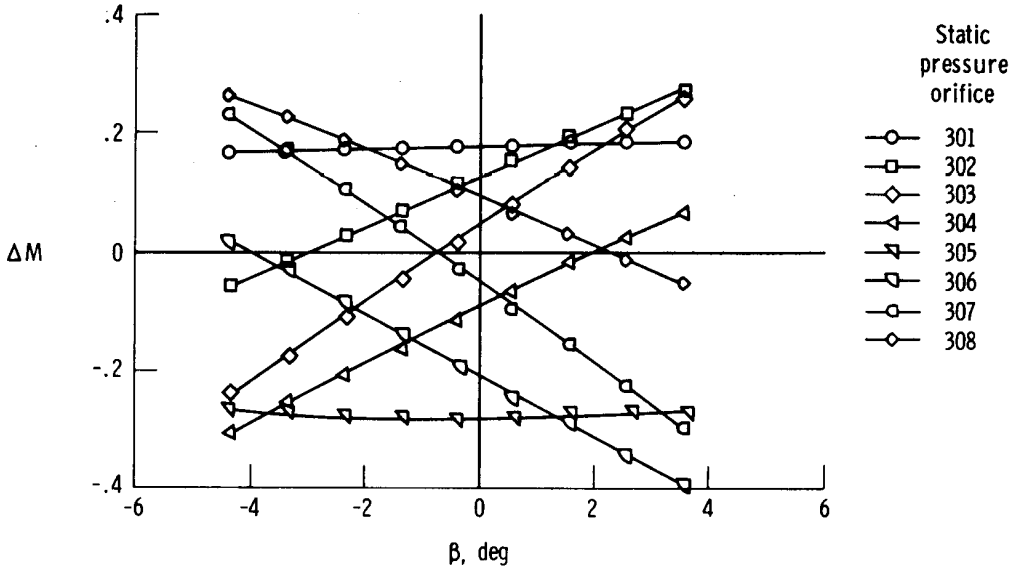

(b) $\alpha \approx 3°$.

Figure 16. Mach number error versus angle of sideslip for the 300-series orifices in tip 2. Sleeve wide open; total pressure tube position = 5.1 cm (2.0 in.); Re ≈ 8.2 × 10⁶ per m (2.5 × 10⁶ per ft).

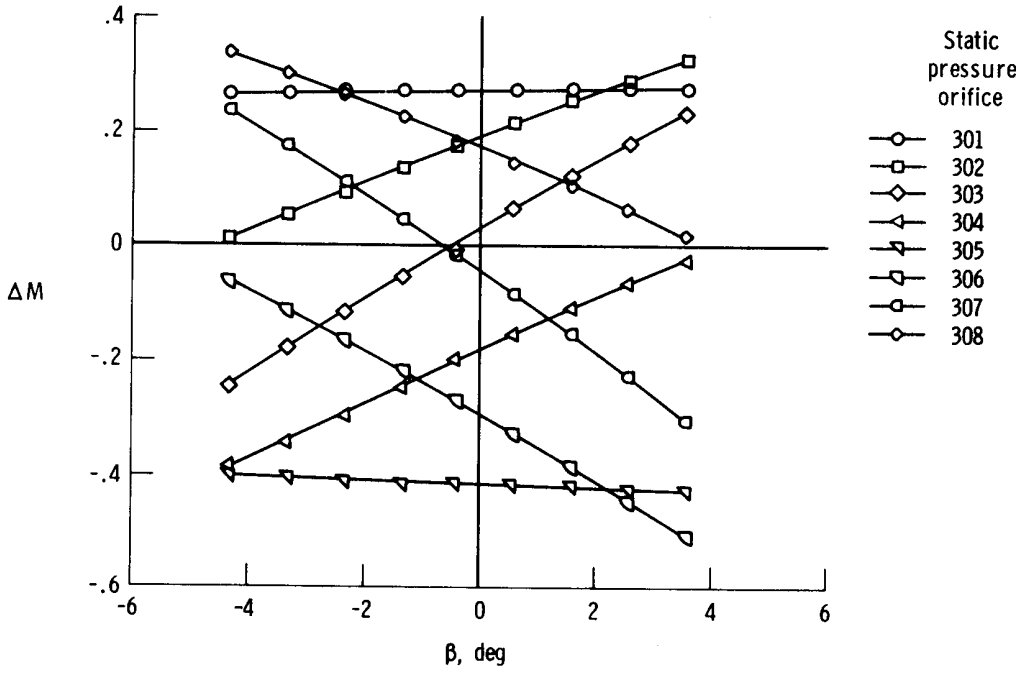

(c) $\alpha \approx 5°$.

Figure 16. Concluded.

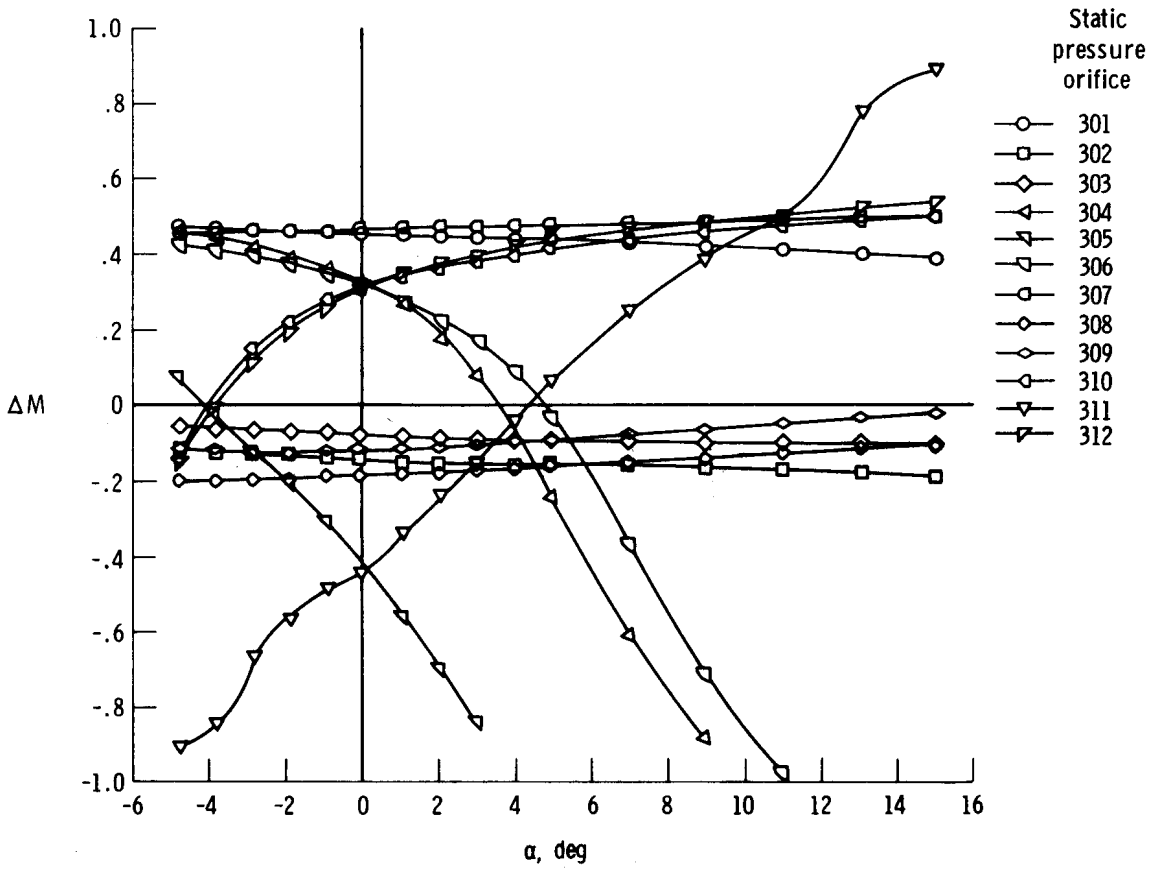

Figure 17. Mach number error versus angle of attack for the 300-series orifices in tip 3. Sleeve wide open; total pressure tube position = 7.5 cm (2.9 in.); Re ≈ 16.4 X 10^6 per m (5 X 10^6 per ft); β ≈ 0°; orifices 301 and 307 oriented in the horizontal plane.

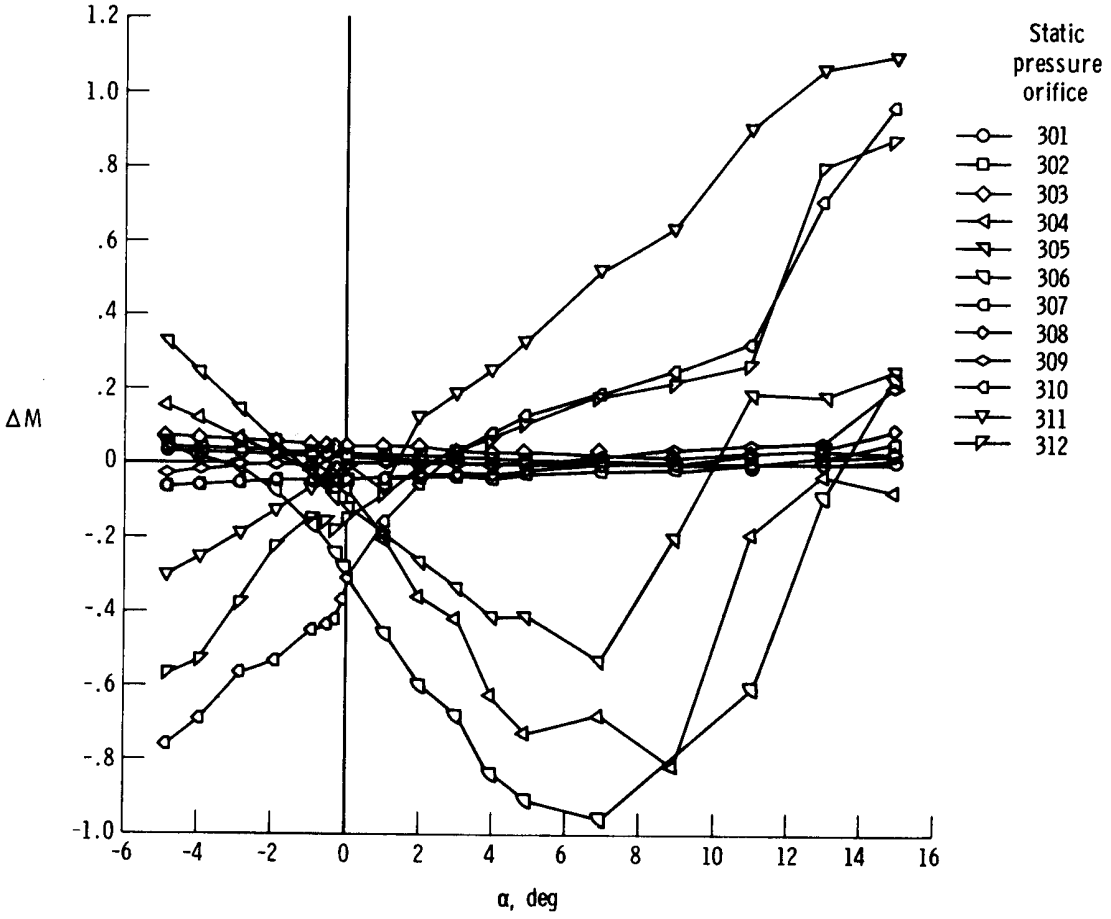

Figure 18. Mach number error versus angle of attack for the 300-series orifices in tip 4. Sleeve wide open; total pressure tube position = 6.6 cm (2.6 in.); Re ≈ 12.4 X 10^6 per m (3.8 X 10^6 per ft); β ≈ 0°; orifices 301 and 307 oriented in the horizontal plane.

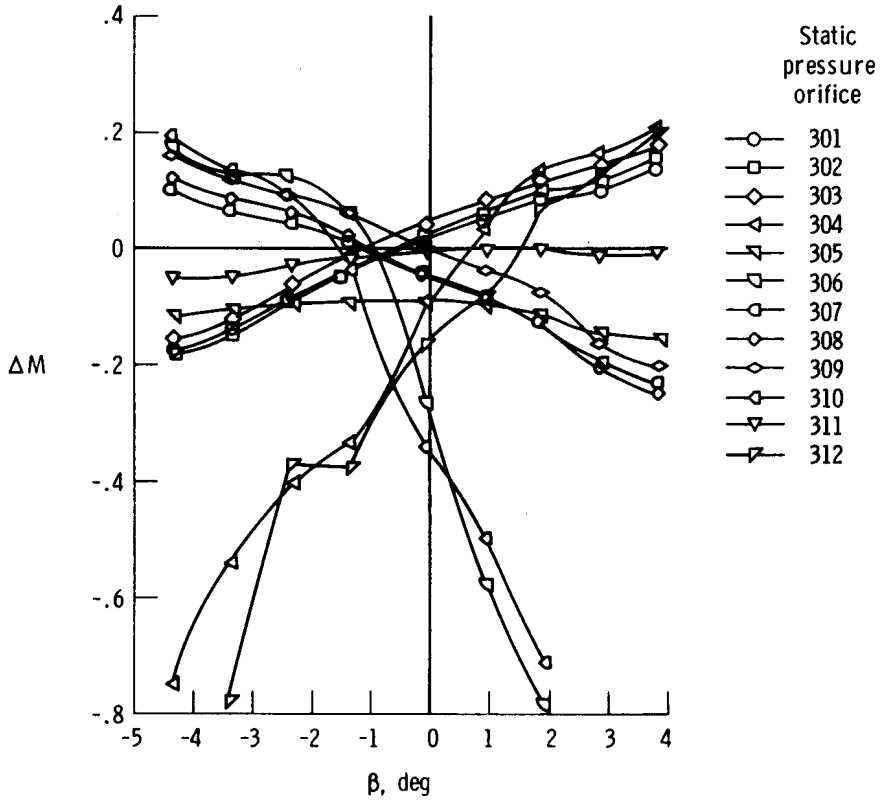

(a) $\alpha \approx 0°$.

Figure 19. Mach number error versus angle of sideslip for the 300-series orifices in tip 4. Sleeve wide open; total pressure tube position = 6.6 cm (2.6 in.); Re ≈ 12.4 × 10⁶ per m (3.8 × 10⁶ per ft); orifices 301 and 307 oriented in the horizontal plane.

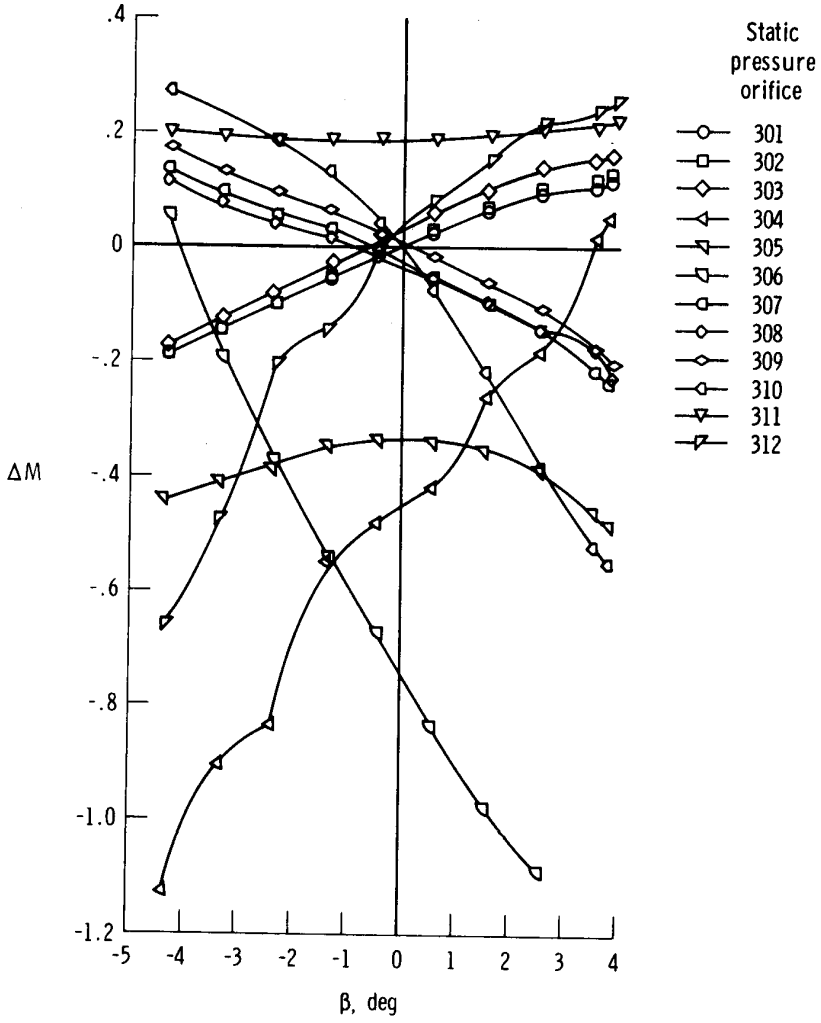

(b) $\alpha \approx 3°$.

Figure 19. Continued.

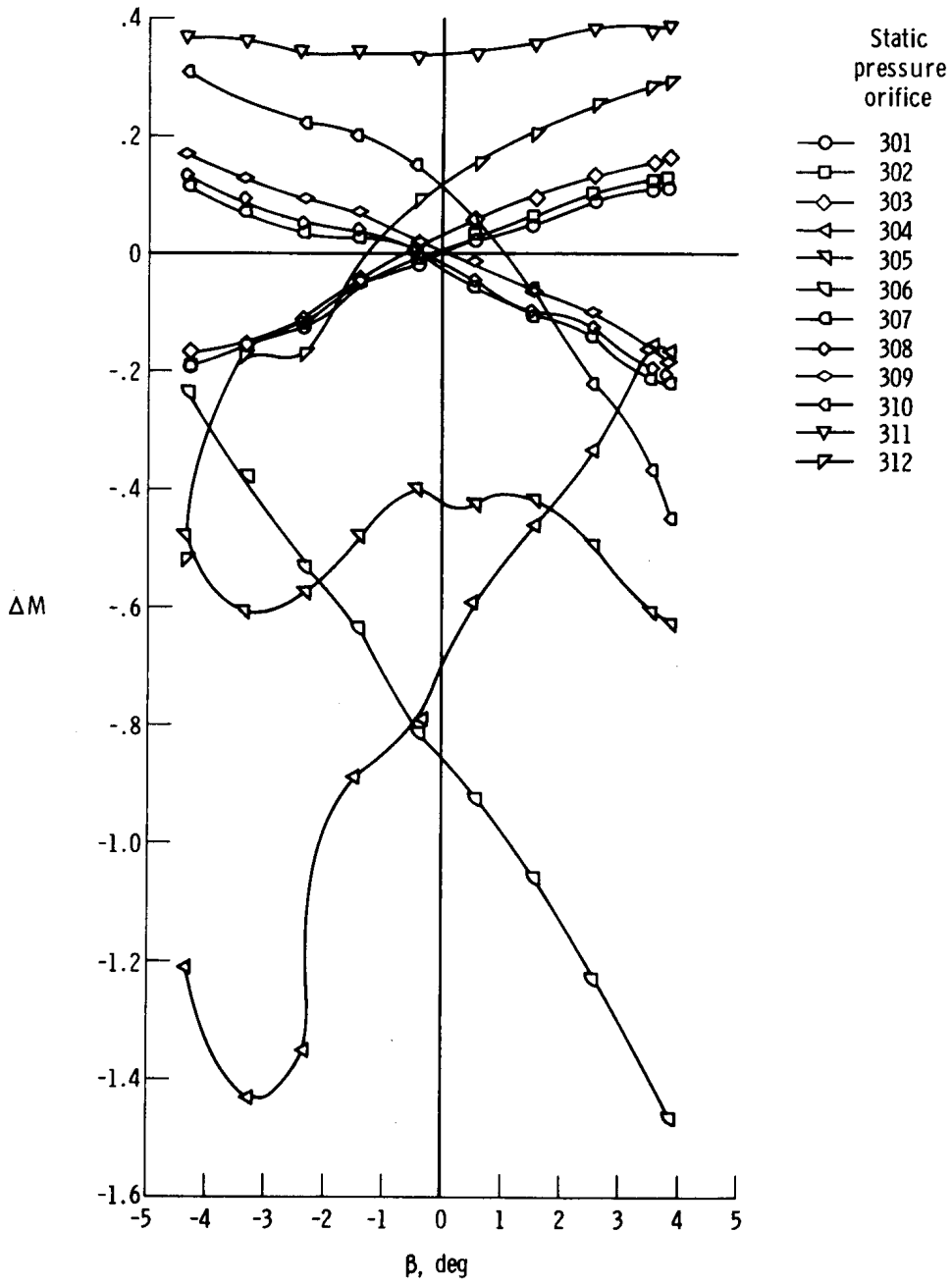

(c) $\alpha \approx 5°$.

Figure 19. Concluded.

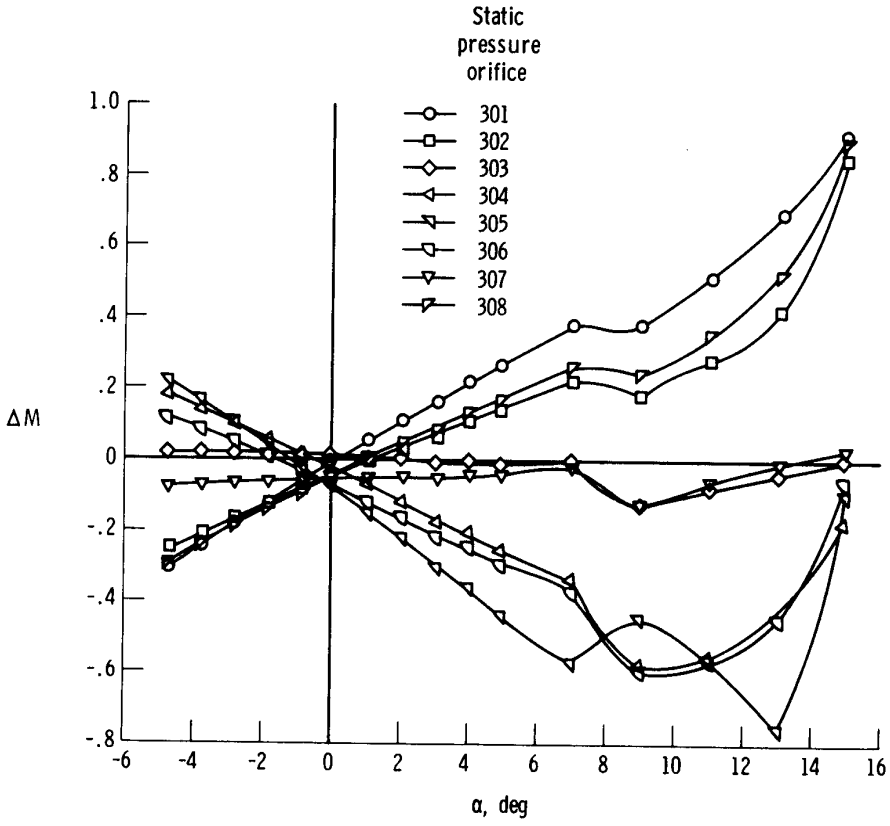

Figure 20. Mach number error versus angle of attack for the 300-series orifices in tip 5. Sleeve wide open; total pressure tube position = 4.0 cm (1.6 in.); Re ≈ 12.4 × 10⁶ per m (3.8 × 10⁶ per ft); β ≈ 0°.

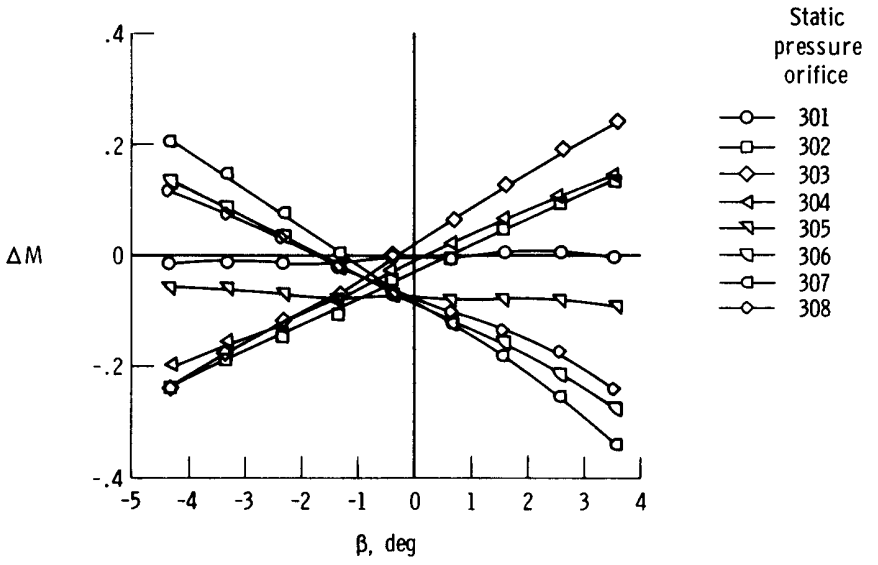

(a) $\alpha \approx 0°$.

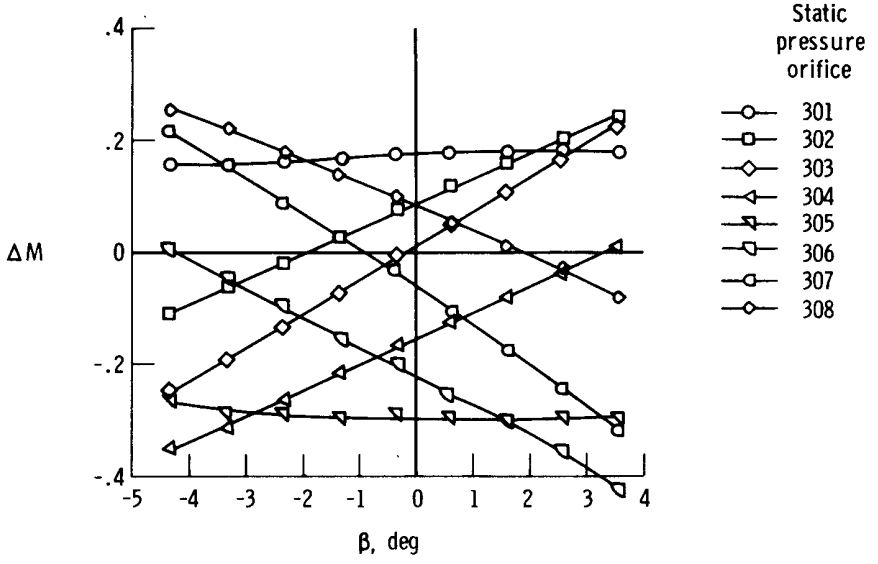

(b) $\alpha \approx 3°$.

Figure 21. Mach number error versus angle of sideslip for the 300-series orifices in tip 5. Sleeve wide open; total pressure tube position = 4.0 cm (1.6 in.); Re ≈ 12.4 × 10⁶ per m (3.8 × 10⁶ per ft).

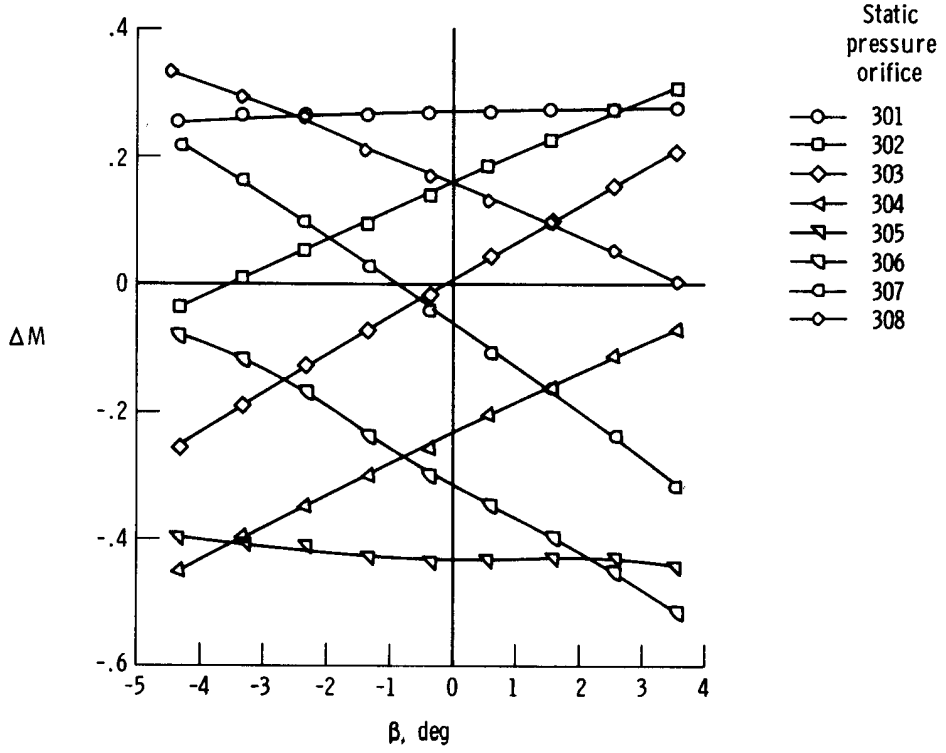

(c) $\alpha \approx 5°$.

Figure 21. Concluded.